Cell Biology

Control of cell retraction and protrusion with a single protein

Reviewed Preprint
v2 • December 11, 2024
Revised by authors

Reviewed Preprint
v1 • November 27, 2023

Jean De Seze, Maud Bongaerts, Benoit Boulevard, Mathieu Coppey

Laboratoire Physico Chimie Curie, Institut Curie, PSL Research University, Sorbonne Université, CNRS UMR168, Paris, France

eLife Assessment

This **important** study combines **compelling** experiments with optogenetic actuation and **convincing** theory to understand how signalling proteins control the switch between cell protrusion and retraction, two essential processes in single cell migration. The authors examine the importance of the basal concentration and recruitment dynamics of a guanine exchange factor (GEF) on the activity of the downstream effectors RhoA and Cdc42, which control retraction and protrusion. The experimental and theoretical evidence provides a model of RhoA's involvment in both protrusion and retraction and shows that these complex processes are highly dependent on the concentration and activity dynamics of the components.

https://doi.org/10.7554/eLife.93180.2.sa3

Abstract

Summary

The ability of a single protein to trigger different functions is an assumed key feature of cell signaling, yet there are very few examples demonstrating it. Here, using an optogenetic tool to control membrane localization of RhoA nucleotide exchange factors (GEFs), we present a case where the same protein can trigger both protrusion and retraction when recruited to the plasma membrane, polarizing the cell in two opposite directions. We show that the basal concentration of the GEF prior to activation predicts the resulting phenotype. A low concentration leads to retraction, whereas a high concentration triggers protrusion. This unexpected protruding behavior arises from the simultaneous activation of Cdc42 by the GEF and inhibition of RhoA by the PH domain of the GEF at high concentrations. We propose a minimal model that recapitulates the phenotypic switch, and we use its predictions to control the two phenotypes within selected cells by adjusting the frequency of light pulses. Our work exemplifies a unique case of control of antagonist phenotypes by a single protein that switches its function based on its concentration or dynamics of activity. It raises numerous open questions about the link between signaling protein and function, particularly in contexts where proteins are highly overexpressed, as often observed in cancer.

Introduction

Cell protrusion and retraction are two morphological changes at the core of various cellular functions, including cell motility, adhesion, and tissue development. For example, during migration the cell must polarize itself by simultaneously controlling two opposite shape changes, protrusion at the front and retraction at the back [1]. Usually, these two morphodynamical events are thought to be spatially and temporally controlled by the segregation of protein activities or component within the cell space. Key controllers of these two processes are the members of the Rho family of small GTPases, in particular the three best known RhoA, Rac1, and Cdc42 [2]. These small proteins act as molecular switches, being turned on in their active GTP form by a large variety of guanine exchange factors (GEFs) and turned off in the GDP form by GTPase activating proteins (GAPs) [3]. Early experiments expressing these GTPases in their active forms [4] led to the canonical picture in which Rac1 and Cdc42 promotes protrusion, with the presence of ruffles and filopodia, while RhoA promotes retraction, as testified by cell rounding and actomyosin contractility.

Yet, a large body of works on the regulation of GTPases has revealed a much more complex picture with numerous crosstalks and feedbacks allowing the fine spatiotemporal patterning of GTPase activities[5]; hereby questioning the legitimacy of the simple canonical picture. This is especially true for RhoA, since it has been proposed to be responsible for both protrusion or retraction depending on the cellular context [6–8]. It thus remains to be addressed whether the induction of protrusions and retractions are simply set by the independent and segregated activities of GTPases or set by a more complicated signal integration.

In recent years, optogenetics has emerged as a very powerful tool to go beyond correlations and to demonstrate causality in this question. Up to now, the optogenetic approaches that have been developed to control GTPases in space and time tended to confirm the canonical picture. For example, we and others have shown that for Rac1 and Cdc42, despite of a complex cross-activation, the recruitment at the plasma membrane of minimal GEF activating domains causally induce cell protrusions [9] and migration led by the front [10]. Along the same line, optogenetic approaches to control RhoA, reviewed in [11] and [12], have all shown a causal induction of cell retraction.

Here, contrarily to previous optogenetic approaches, we report a serendipitous discovery where the optogenetic recruitment at the plasma membrane of GEFs of RhoA triggers both protrusion and retraction in the same cell type, polarizing the cell in opposite directions. In particular, one GEF of RhoA, PDZ-RhoGEF (PRG), also known as ARHGEF11, was most efficient in eliciting both phenotypes. We show that the outcome of the optogenetic perturbation can be predicted by the basal GEF concentration prior to activation. At high concentration, we demonstrate that Cdc42 is activated together with an inhibition of RhoA by the GEF leading to a cell protrusion. Thanks to the prediction of a minimal mathematical model, we can induce both protrusion and retraction in the same cell by modulating the frequency of light pulses. Our ability to control both phenotypes with a single protein on timescales of second provides a clear and causal demonstration of the multiplexing capacity of signaling circuits.

Results

Local optogenetic recruitment to the plasma membrane of a DH-PH domain of RhoA GEF can lead

to both protrusion and retraction in single cells

To control the activity of RhoA in migrating cells, we developed optogenetic tools based on the iLID-SspB light-gated dimerization system to recruit activating domains of GEFs specific to RhoA (**Figure 1A**). Using a strategy already applied to other GTPases [13] and to RhoA itself [14], we anchored the iLID part of the dimer to the membrane thanks to a CAAX motif together with the fluorescent protein mVenus, and expressed in the cytosol the DH-PH domains of different GEFs of RhoA fused to the SspB protein (**Figure 1B**). We cloned the iLID-SspB dimers into a plasmid separated by a P2A motif so that they were expressed at a one-to-one ratio. We selected three of the best-known GEFs of RhoA: LARG (ARHGEF12), GEF-H1 (ARHGEF2), and PDZ-RhoGEF (ARHGEF11). The LARG DH domain was already used with the iLid system [15], the GEF-H1 DH domain had been recruited by optochemical methods [16], and PRG was used with the CRY2-CIBN system [17]. We chose to add the PH domains of GEFs in our constructs since it participates to an auto-amplification process [18] and appears to be sometimes required for GEF specificity [19]. All strategies developed so far have been shown to trigger cell contractility, either in single cells or in monolayers.

We then transiently transfected RPE1 cells with our optogenetic systems (henceforth called optoPRG, optoLARG, and optoGEF-H1) and examined the effects of pulsatile local activation done thanks to a digital micromirror light source (see material and methods). In all cases, we saw a clear recruitment of the cytosolic part to the plasma membrane, between 3 and 10 fold, depending on the transfection intensity and the amount of light sent to the sample.

To our surprise, recruitment of DH-PH domains of the three GEFs of RhoA to the membrane with the same experimental procedure resulted in very different phenotypes (**Figure 1C,D** and Supp Movie 1-2). Whereas the optoLARG elicited only the expected retractile phenotype typical of RhoA pathway (Supp Movie 2), optoGEF-H1 and optoPRG exhibited less predictable behavior (**Figure 1D**). The retractile phenotype was observed in many cells, but a large proportion of cells showed a seemingly opposite response, namely a clear protruding phenotype with filopodia and ruffles (**Figure 1C**). For optoGEF-H1, most of the cells were very round after transfection and showed no response at all after optogenetic recruitment of the DH-PH domain to the membrane. Only few cells (~40%) showed distinct morphological changes after activation, most of them retracted, but some also showed a clear protruding phenotype (Supp Movie 2). For optoPRG, most cells showed a distinct phenotypic response upon blue light exposure (**Figure 1D**). Almost 35% of the cells exhibited a clear retracting phenotype leading to the formation of blebs or protrusions at the other side of the cell (Supp Movie 1), while 40% exhibited a markedly protruding phenotype (Supp Movie 1), reminiscent of the effect of an optoGEF for Cdc42 or Rac1 [9] and often leading to retraction of the other non-activated pole of the cell. A small fraction of cells (~10%) showed no clear response, and the remaining cells (~25%) showed a mixed phenotype: while we could see ruffles or filopodia forming at the site of activation, the cell did not move and appeared to contract at the same time, leading to blebs at the other pole of the cell (Supp Figure 1A).

To classify the different phenotypes in an unbiased manner, we computed the evolution of the membrane area inside the activation square during the activation with (**Figure 1E**) or without light (**Figure 1F**). We could see the clear impact of the recruitment of the optoPRG, that either triggers a diminution of membrane area -a retraction- or an increase in membrane area -a protrusion-, while control cells show a much smaller membrane movement over the time course of the experiment. Quantification of the changes in membrane area in both the activated and non-activated part of the cell (Supp Figure 1B-C) reveals that the whole cell is moving, polarizing in one direction or the other upon optogenetic activation.

To ensure that the cell response was not due to an already set polarity, we repeated the activation at the other pole of the cell one hour after the first round of activation, when cells had recovered from the first activation and were back to a resting state. Almost all cells retained the same phenotype: they protruded when they were already protruding and retracted when they were

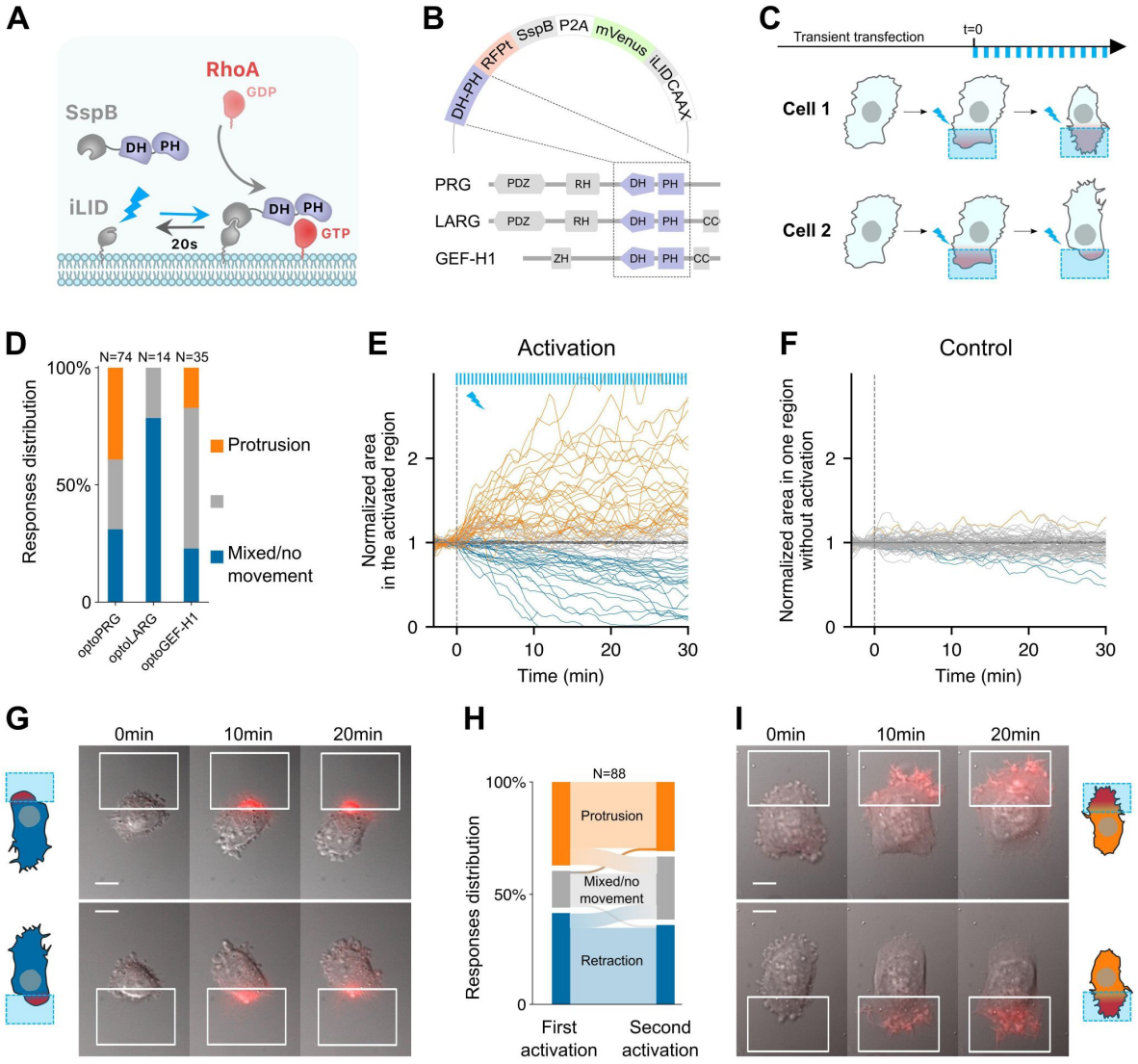

Figure 1

optogenetic activation of RhoA leads to protrusion or retraction.

(**A**) Scheme of the optogenetic tool. Optogenetic dimer (in gray) dimerizes upon blue light activation (blue arrow), and dissociates in the dark with an off rate of 20s (black arrow). DH-PH domain is fused to the SspB moiety (purple), which recruitment to the plasma membrane through iLID triggers RhoA activation, from GDP (light red) to GTP (dark red) state. (**B**) The three opto plasmids, with DH-PH domains (purple) shown in their wildtype position in the different RhoA GEFs used here. (**C**) Experimental timeline. Transient transfection is done at least 30 hours before local activation (blue squares). Activation is done by pulses (blue bars, top) at different frequencies, intensities and durations. Cells are observed for 30 to 60 minutes. (**D**) Responses distributions for each optogenetic tool. (**E**,**F**) Area over time of the cell in the activated region (**E**) or without activation (**F**), normalized by the mean initial area. t=0 is the starting point of the activation, each blue bar on top representing one light impulse. Orange: protruding cells, blue: retracting cells, gray: nonmoving cells or mixed phenotype (labeled by hand). (**G**,**I**) representative cells doing retraction (on the left) and protrusion (on the right) upon optogenetic activations on two different side of the cell. Scale bar: 10 µm. White squares: area of activation. Red color: RFPt channel (optogenetic tool). (**H**) Sankey diagram representing the proportion of cells doing a protrusion (orange), retraction (blue) or a mixed phenotype (gray) at one side (first activation) or the other side (second activation).

already retracting (**Figure 1G-I**). Only few cells showed a mixed phenotype in the first or second round, whereas their phenotype was clear for the other round (**Figure 1H**). Thus, we concluded that for one type of optogenetic activation (one frequency and one light intensity), the phenotype triggered by the recruitment of the optoPRG to the membrane was determined by the state of the cell and not by the cell section in which the optogenetic activation was performed.

To further verify that these opposite phenotypes were not cell line specific, we performed the experiment in Hela cells. The two phenotypes could be observed after transient transfection with optoPRG and activation with the same protocol (Supp Figure 1D-E), showing that these two opposites phenotypes are not restricted to RPE1 cells only. Thus, the DH-PH domain of PRG can induce both retraction and protrusion upon its recruitment in single cells. These opposite phenotypes occur in the same cell line, in the same biomechanical environment, and with the same dynamics of recruitment to the membrane. This dual behavior is not cell-specific or exclusive to this GEF of RhoA, as it has also been observed with GEF-H1, although with much less efficiency. For the rest of our study, we focused on optoPRG that elicits the strongest and most reproducible opposing phenotypes.

Cell phenotype upon optogenetic activation depends on the cytosolic concentration of exogenous optoPRG

We next wonder what could differ in the activated cells that lead to the two opposite phenotypes. As all the experiments above were done by transiently transfecting cells, the cell- to-cell variability of expression led to a wide range of cytosolic concentrations of optoPRG that we can estimate by measuring the mean fluorescence intensity. Looking at the area in the activated region after 5 minutes against the cytosolic concentration of optoPRG leads to very clear result (**Figure 2A**). Below a specific concentration threshold (~40 a.u.), almost all the activated cells (~95%) retract their membrane within the activation area, while above this threshold, ~85% of the cells extend their membrane (see **Figure 2B** for selected examples). This result clearly demonstrates that the phenotype triggered by the activation of optoPRG can be predicted by its concentration within the cell before activation.

This leads to two hypotheses. Either the cell is responding to differences in the absolute amount of optoPRG recruited at the membrane, or the cell is in a different state before optogenetic activation that leads to opposite responses to optoPRG activation. To exclude one of these hypotheses, we first looked at the absolute recruitment at the membrane (**Figure 2C**). Even if the absolute recruitment depends on the initial concentration, we saw a lot of retracting cells reaching very high absolute optoPRG recruitment levels, which tends to exclude the first hypothesis. To further demonstrate it, we overexpressed in a different fluorescent channel a non-recruitable DH-PH domain of PRG, together with the optoPRG, in order to decouple global and recruited PRG concentration. We saw that overexpressing PRG DH-PH strongly increased the number of protruding phenotypes in low expressing cells (from 0% to 45%, **Figure 2D**, compare also with **Figure 2A**). Moreover, it was clear that the phenotype switch also correlates with the initial concentration of overexpressed PRG DH-PH domain, highly expressing cells being more prone to protrude (orange dots on the left, **Figure 2D**).

Most optogenetic tools that control GTPases activity rely on the fact that GEF domains are less active in the cytosol. Here, the phenotype switch is dictated by the amount of over-expressed optoPRG. Thus, PRG DH-PH domain must have some activity before optogenetic recruitment to the membrane, changing protein basal activities and/or concentrations - which we called the cell state. To confirm that cells were in a different state, we first measured the average cell area before activation in the two phenotypes, and saw a strong and significant difference, highly expressing cells being 1.5 times bigger than low expressing cells (Supp Figure 2). We then looked at

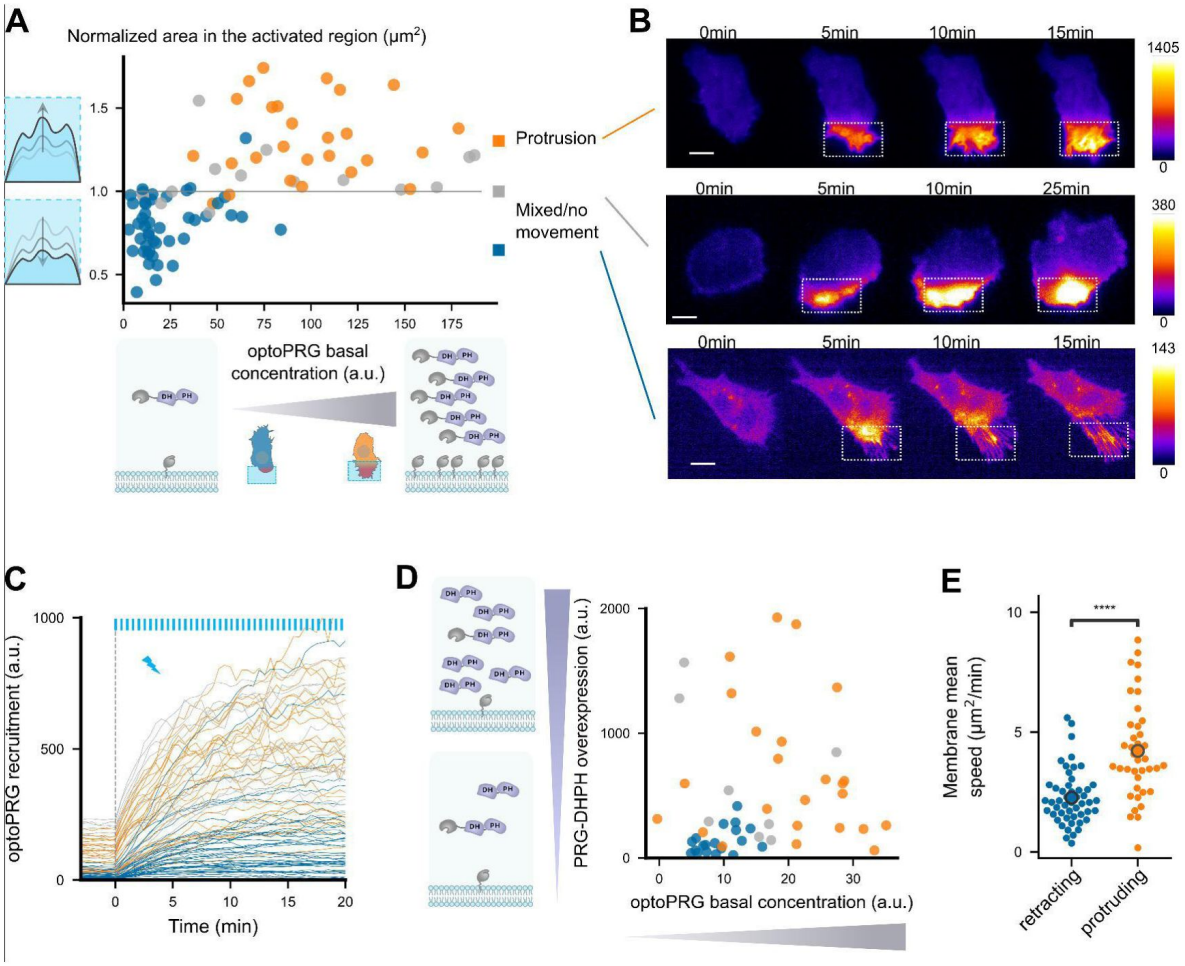

Figure 2

cell phenotype depends on the initial optoPRG concentration.

(A) Phenotype dependence on initial cytosolic optoPRG concentration. The normalized area in the activated region after 5 minutes is plotted against the mean fluorescence intensity for each cell, which color is labeled by hand depending on the observed phenotype. Schemes on the bottom represent high and low levels of expression (P2A plasmids implies approximately a one-to-one ratio of iLID against SspB). **(B)** Three representative time lapse images of transiently transfected cells, one retracting (top), one showing a mixed phenotype (middle), and one protruding (bottom). Intensities are very different, as seen by the dynamic range of the colormaps presented on the right. (**C**) Absolute fluorescence intensity of recruited optoPRG, before (t<0) and after (t>0) activation. Blue bars: activation pulses. (**D**) Phenotype depending on both optoPRG concentration and PRG DH-PH overexpression, measured both by fluorescence intensity (a.u.). Increasing recruitable and non-recruitable DH-PH domain of PRG both lead to protruding phenotypes. Phenotypes are manually labelled. (**E**) Membrane mean absolute displacement to compare membrane activity between retracting (blue) and protruding (orange) cells. (Mann–Whitney U test. **** <0.0001)

membrane ruffles without any optogenetic activation, by calculating the mean absolute speed of membrane displacement in one region. We also observed a significant difference, protruding cells having more and stronger membrane displacements before being activated (**Figure 2E**).

This series of experiments led us to the conclusion that the main determining factor of the phenotype is the cytosolic concentration of the DH-PH domain of PRG before the optogenetic activation. This initial concentration changes the cell state, in a way that the recruitment of the DH-PH domain of PRG triggers opposite cellular responses.

Two distinct signaling pathways are triggered from the first activation timepoint

Very surprised by this ability of one protein to trigger opposite phenotypes, we sought to further characterize these responses by monitoring the activity of key proteins involved in the RhoA pathway. To this end, we initially investigated whether the variation in actin and myosin levels following optogenetic activation corresponded to the stereotypical dynamics of protrusions and retractions described in a previous study by Martin *et al.* [20]. We thus monitored Lifeact-iRFP and MRLC-iRFP (Myosin regulatory light chain) proteins during the optogenetic experiments. In the retraction phenotype, the first recruitment of optoPRG to the membrane was followed by an immediate polymerization of actin in the area of activation, as we quantified over multiple experiments (**Figure 3A-C**). Myosin recruitment appeared to follow the polymerization of actin, leading to the retraction of the membrane in the minutes following the activation (**Figure 3D-F**). In contrast, when cells were protruding, we observed a decrease in MRLC and Lifeact intensities following the first activation of our tool by light (**Figure 3A-F**), as it was previously shown for protrusions triggered by PDGF [20]. This first decrease is probably due to the depolymerization of stress fibers at the area of activation. It is followed by an increase in actin polymerization, most probably responsible for the net displacement of the membrane, while myosin stays lower than the initial state. These differences in actin and myosin dynamics for the two phenotypes are visible at 30 seconds, one frame after the first pulse of light (**Figure 3C,F**), even if the cell phenotype cannot be distinguished by eye before one or two minutes. This shows that the pathways triggered by optoPRG recruitment differs from the first tens of seconds after light activation. We thus turned to RhoA itself, which is supposed to be upstream of actin and myosin, and just downstream of PRG. As our optogenetic tool prevented us from using FRET biosensors because of spectral overlap, we turned to a relocation biosensor that binds RhoA in its GTP form [21]. This highly sensitive biosensor is based on the multimeric TdTomato, whose spectrum overlaps with the RFPt fluorescent protein used for quantifying optoPRG recruitment. We thus designed a new optoPRG with iRFP, which could trigger both phenotypes but was harder to transiently express, giving rise to a majority of retracting phenotype. Looking at the RhoA biosensor, we saw very different responses for both phenotypes (**Figure 3G-I**). While retracting cells led to strong and immediate activation of RhoA, protruding cells showed a much smaller and delayed response. After the first minute of optogenetics activation, no significant change was seen in protruding cells (**Figure 3I**). Thus, either an unknown factor is sequestering RhoA-GDP, or optoPRG preferentially binds to another partner, both hypotheses being non-mutually exclusive.

Altogether, these data demonstrate that cells exhibit very different responses to optoPRG activation, regarding both actin polymerization and myosin activity, and even RhoA activity itself. They show that different pathways are immediately engaged, already at the level of Rho-GTPases, few tens of seconds after the first optogenetic activation.

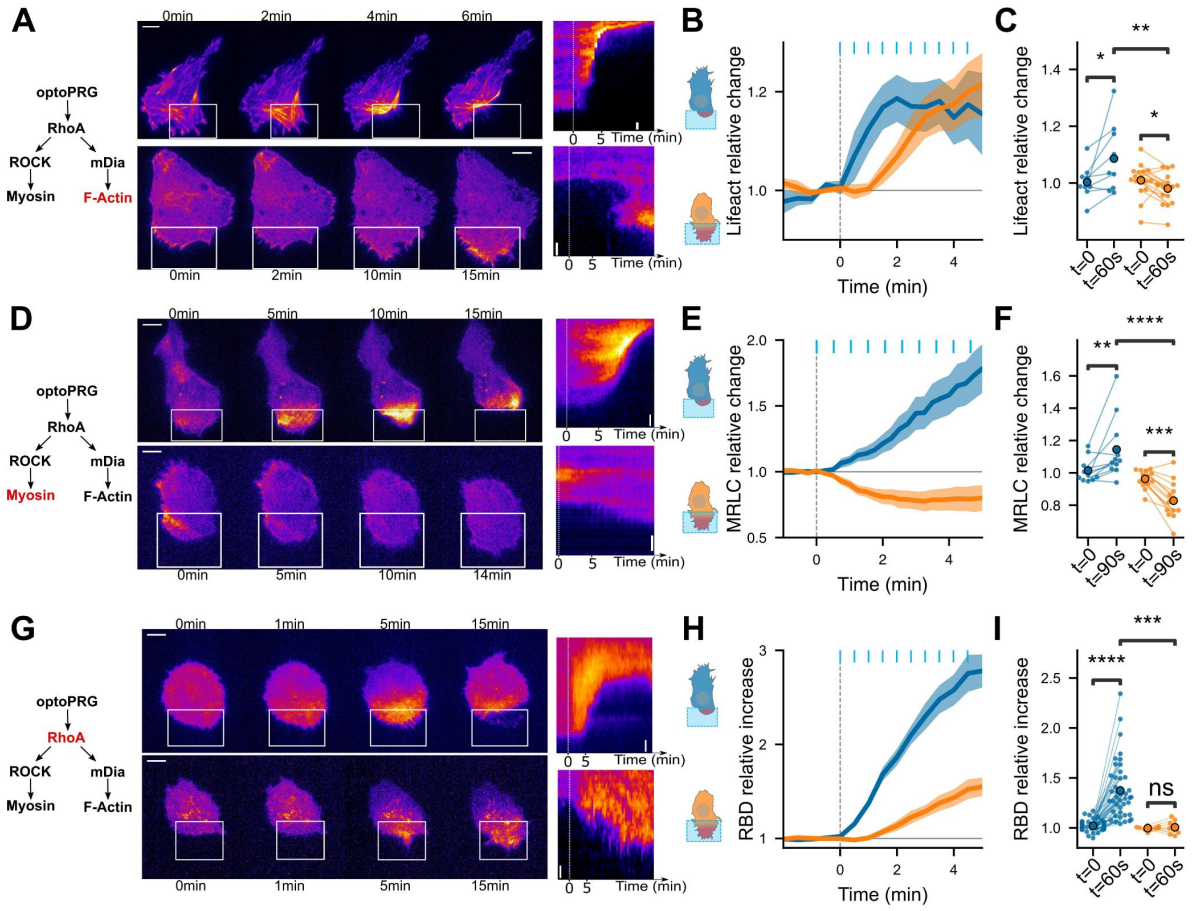

Figure 3

Downstream effectors show that cell phenotype is set immediately.

Distinct pathways are triggered from the first timepoint. (**A**,**D**,**G**) Representative timelapse images and kymographs of retracting (top) and protruding (bottom) cells labeled with Lifeact-iRFP (**A**), MRLC-iRFP(**D**), and RBD-2xTdTomato biosensor (**G**), activated with optoPRG starting at t=0min. White rectangles are areas of optogenetic activation. Scale bars are 10 µm. (**B**,**E**,**H**) Corresponding mean normalized intensities are plotted against time (mean +/- s.e.m.), blue for retracting cells and orange for protruding one. (**C**,**F**,**I**) Corresponding pairwise comparison for each cell of the signal inside the region of activation between the initial time and 60s (Lifeact-iRFP and RhoA biosensor) or 90s (MRCL-iRFP). Data are grouped by phenotype. *P<0.05 **P<0.01, ***P<0.001, **** P<0.0001 (Wilcoxon test to compare t=0 and t>0, independent t- test otherwise)

PH domain of PRG can inhibit RhoA and is necessary for the protruding phenotype

As the phenotype triggered by optoPRG, revealed on a minute timescale, seems to be set by the reactions of the intracellular biochemical network after few tens of seconds, we turned to an analysis of RhoA activity at smaller timescale. Our first surprise came while looking at the response of the RhoA biosensor to pulses of optoPRG activation. We show in **Figure 4A** three representative examples of such responses. While at low optoPRG concentration (cell 1), RhoA activity follows the pulses of optoPRG with some delay, at higher concentrations (cell 2 and cell 3), RhoA activity shows a very different behavior: it first decays, and then rises. It seems that, adding to the well-known activation of RhoA, PRG DH-PH can also negatively regulate RhoA activity.

Knowing that the PH domain of PRG triggers a positive feedback loop thanks to its binding to active RhoA [18], we hypothesized that this binding could sequester active RhoA at high optoPRG levels, thus being responsible for its inhibition. To test our hypothesis, we designed a new optogenetic tool to recruit only the PH domain of PRG (called optoPH), while looking at the basal RhoA activity. In some cells, we could see a very clear immediate decrease of the biosensor intensity following optoPH recruitment, very similar in terms of dynamics to the decrease observed in highly expressing cells (**Figure 4B-D**). This decrease was significant on the mean but not clearly visible in all cells (Supp Figure 3), which was expected since the PH inhibition should depend strongly on the basal RhoA activity that might be mild in resting cells. Our result confirmed that the PH domain of PRG alone can inhibit RhoA activity, probably through a direct binding as proposed in [18] (**Figure 4D**).

Next, we wondered whether such an inhibition plays a role in the protruding phenotype we observe with optoPRG. To test this, we mutated our optoPRG with a double mutation (F1044A and I1046E) known to prevent binding of the PH domain of PRG to RhoA-GTP [18]. This dual mutation had a strong effect on our optogenetic activations, restricting the phenotypes to only the retracting ones, even at high basal concentrations (**Figure 4E,F**). We concluded that the PH domain of optoPRG must bind to RhoA-GTP for the protruding phenotype to happen; either before the activation - to change the cell state - or during recruitment - to prevent RhoA activity. To discriminate between these two hypotheses, we overexpressed the DH-PH domain alone in another fluorescent channel (iRFP) and recruited the mutated PH at the membrane. If the binding to RhoA-GTP was only required to change the cell state, we would expect the same statistics than in **Figure 2D**, with a majority of protruding cells due to DH-PH overexpression. On the contrary, we observed majority of retracting phenotype even in highly expressing cells (**Figure 4G**), showing that the PH binding to RhoA-GTP during recruitment is a key component of the protruding phenotype. Few cells with very high PRG concentration still displayed small ruffles, indicating that even if much less efficient, optoPRG with mutated PH could still trigger protrusions.

These experiments suggest a necessary role of the PH domain of optoPRG for protrusions, but is it sufficient? To check this, we looked at the phenotypic response of cells that overexpress PRG, where we only recruit the PH domain. We could not see either clear protrusion or retraction happening following PH recruitment, as shown by membrane displacement in **Figure 4H,I**. Thus, the inhibitory function of the PH domain is not sufficient for triggering protrusions. This points to the activation of another effector, actively responsible for protrusion formation.

optoPRG activates Cdc42

To find the active process involved in the protruding phenotype, we turned to the two other best-known GTPases, Rac1 and Cdc42, which are main drivers of cell protrusions. Indeed, a recent work showed that the DH-PH domain of PRG was able to bind Cdc42 and activate it, thanks to conformational change operated by $G\alpha_S$ [22]. To look at the dynamic activity of Rac1 and Cdc42, we first used a Pak Binding Domain (PBD) fused to iRFP. PAK is known for being an effector of both

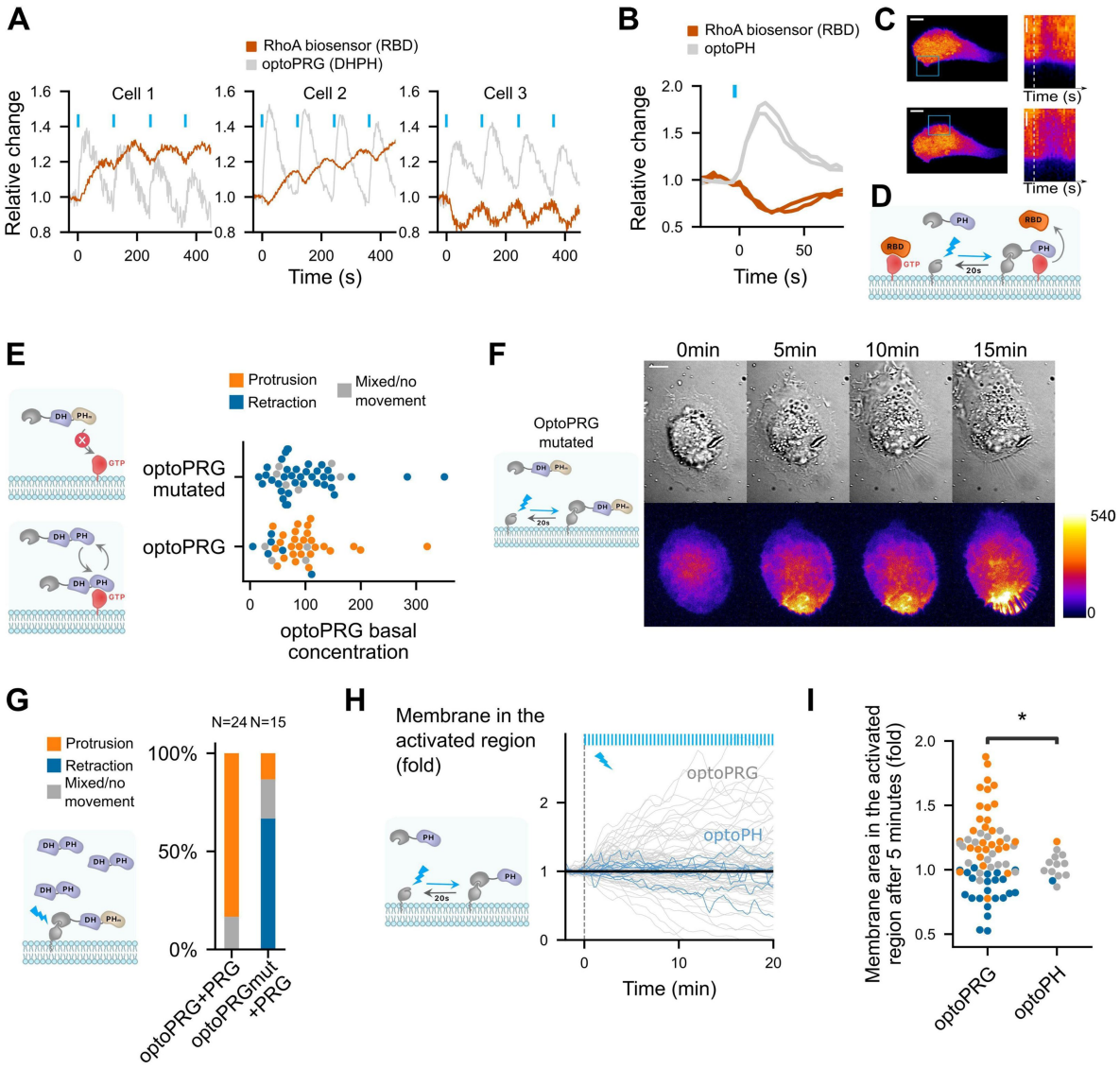

Figure 4

PH domain of PRG is triggering inhibition of RhoA at high PRG concentration and is necessary but not sufficient for protruding phenotype.

(**A**) Three representative cells that show very different responses to optoPRG pulsatile activation. Cell 1 has a low optoPRG expression, while Cell 2 and Cell 3 have high concentration of optoPRG. Intensities are normalized by the mean intensity before the first activation (t=0). (**B**) Quantification of the relative change in RhoA biosensor (RBD) after one pulse of optogenetic recruitment of the PH domain of PRG. In gray, optoPH recruitment, in red, RhoA biosensor. Light pulses are shown with blue bars. (**C**) Image of the corresponding cell. On the right, kymograph taken within the activation region. White dotted line shows the starting point of the activation. Scale bar: 10 µm. Region of activation is shown is the blue rectangle. (**D**) Scheme of the probable mechanism of PH domain dominant negative effect on RhoA. **(E)** Phenotype after optogenetic activation for optoPRG (bottom) and optoPRG with the PH mutated for no binding to RhoA-GTP (top). On the left, schemes of the expected behavior of the corresponding proteins. (**F**) Representative image of a cell transfected with the optoPRG with mutated PH, doing a retraction despite the high optoPRG concentration. (**G**) Quantification of protruding and retracting phenotypes in cells highly overexpressing non-recruitable PRG, comparing mutated and non-mutated optoPRG, with a scheme of the experiment on the left. See Supp Figure 3 for the selected cells. (**H**) Membrane displacement of optoPH cells (in blue) with overexpressed DH-PH domain of PRG, compared to optoPRG cells (in gray). No specific protrusion can be seen. (**I**) Normalized membrane area after 5 minutes in the activated for optoPRG and optoPH cells. Orange: protruding cells, gray: mixed phenotype or no movement, blue: retracting cells.

Rac1 and Cdc42, but more sensitive as a biosensor of Cdc42 [23]. After optogenetic activation, we saw an increase in PBD intensity in both the protruding and retracting phenotypes. After one minute, PBD intensity continuously increases for the protruding phenotype while it remains unchanged for the retracting phenotype (**Figure 5A-C**). This suggested an immediate activation of Rac1 or Cdc42 after recruitment of optoPRG, that would be inhibited after few minutes in the case of the retracting phenotype.

We then turned to recently published biosensors that are more specific to Rac1 and Cdc42 [24]. It revealed that Cdc42 is the Rho-GTPase specifically activated immediately after optogenetic activation (**Figure 5D-F**), Rac1 being activated afterwards and only in the protruding phenotype (**Figure 5G-I**), most probably due to the positive feedback between Cdc42 and Rac1 [9]. It also confirmed that Cdc42 was activated in both phenotypes just after the optogenetic recruitment but kept being activated only in the case of the protruding phenotype.

To confirm that Cdc42 activation was necessary for the protrusion, we performed an experiment with IPA3, a drug targeting PAK, one of the direct effectors of Cdc42. We did a first optogenetic activation with a set of cells to know their phenotypes, then incubated our sample five minutes with 5 µM IPA3 and activated the cells again (**Figure 5J**). A lot of cells became round, and none of them were able to protrude again upon optogenetic activation, while retracting ones were often still able to retract (**Figure 5K**). Some previously protruding cells were even able to change phenotype and retract after drug incubation (**Figure 5J,K**). This confirmed us that activation of PAK through Cdc42 was required for the protruding phenotype to happen, but not for the retracting one.

An effective model recapitulates RhoA activity dynamics and enables a control of both phenotypes in the same cell

Given the complexity of all interactions happening and the quantitative nature of our findings, we sought a minimal model that would capture RhoA biosensor dynamics and the phenotype switch as a function of optoPRG basal concentration. We also wanted to see if we could play with the quantitative properties of the light stimulation to control both phenotypes in the same cell.

To model RhoA dynamics within a region of the cell, we considered a simple reaction scheme (**Figure 6A**) where inactive RhoA is activated by the GEF (optoPRG) following mass action kinetics. The GEF can be either free or bound to active RhoA thanks to its PH domain. This complex between RhoA-GTP and the GEF, noted *GR*, is inhibiting RhoA downstream activity by titrating active RhoA but does not prevent GEF activity, as shown in [18]. The formation of the complex is characterized by the dissociation constant K_b. Active RhoA is assumed to be deactivated by endogenous GAP at a rate k_2, which sets the characteristic delay between GEF and RhoA-GTP dynamics, putting aside the formation of the complex *GR*. During an optogenetic activation, we assumed that the amount of the GEF, called G_{tot}, is changing because of local concentration increase by membrane recruitment. Introducing the dimensionless variables $r = R/R_{\text{eq}}$ and $g = G_{\text{tot}}/G_{\text{eq}}$, G_{eq} and R_{eq} being the values at equilibrium, and making a quasi-steady state approximation (see Supp Note for a detailed derivation of the model) we obtain the following main equation for the relative evolution of actively signaling RhoA:

$$\frac{dr}{dt} = \frac{1}{1+\frac{G_{\text{eq}}}{K_b}\cdot g}\left(k_2(g-r) - \frac{G_{\text{eq}}}{K_b}\cdot r\frac{dg}{dt}\right).$$

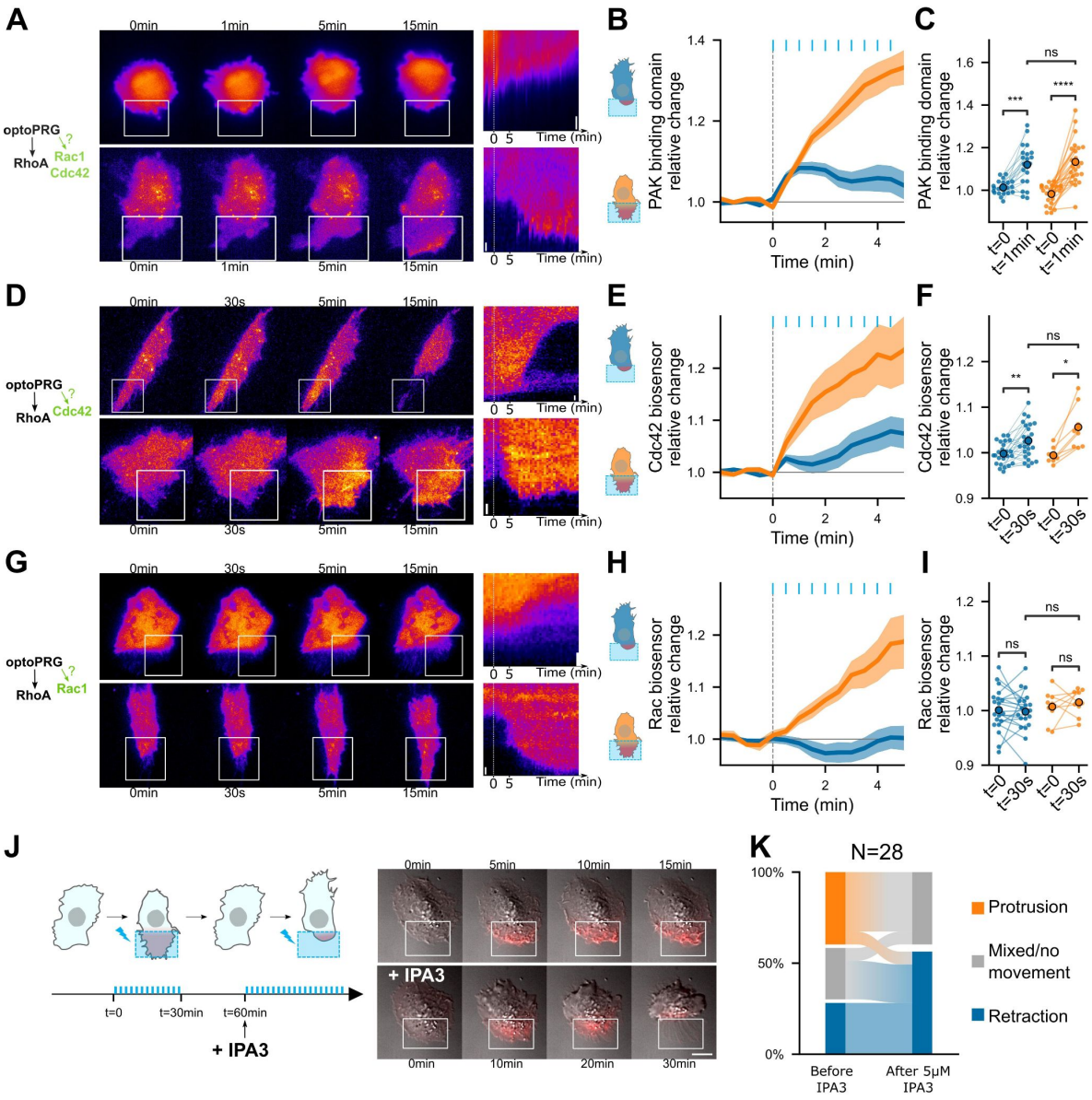

Figure 5

PRG activates Cdc42 and Cdc42 downstream activity is necessary for the protrusive phenotype.

(A,D,G) Representative time-lapse images and kymographs of retracting (top) and protruding (bottom) cells labeled with PBD-iRFP (**A**), delCMV-mCherry-WaspGBD (**D**), and mCherry-3xp67Phox (**G**) biosensors [24], activated with optoPRG starting at t=0min. White rectangles are areas of optogenetic activation. Scale bars are 10 µm. (**B,E,H**) Corresponding mean normalized intensities are plotted against time (mean +/- s.e.m.), blue for retracting cells and orange for protruding one. (**C,F,I**) Corresponding pairwise comparison for each cell of the signal inside the region of activation between the initial time and 60s (PBD biosensor) or 30s (Cdc42 and Rac1 biosensors). Data are grouped by phenotype. *P<0.05 **P<0.01, ***P<0.001, **** P<0.0001 (Wilcoxon test to compare t=0 and t>0, independent t- test otherwise). (**J**) Left, scheme describing the IP3 experiment. Blue bars represent optogenetic pulses (every 30s). Half an hour after the first experiment, IPA3 is added at 5 µM. Right, representative cell showing a protruding phenotype with ruffles (top), and a retracting phenotype after addition or IPA3 (bottom). (**K**) Quantification of phenotype switches.

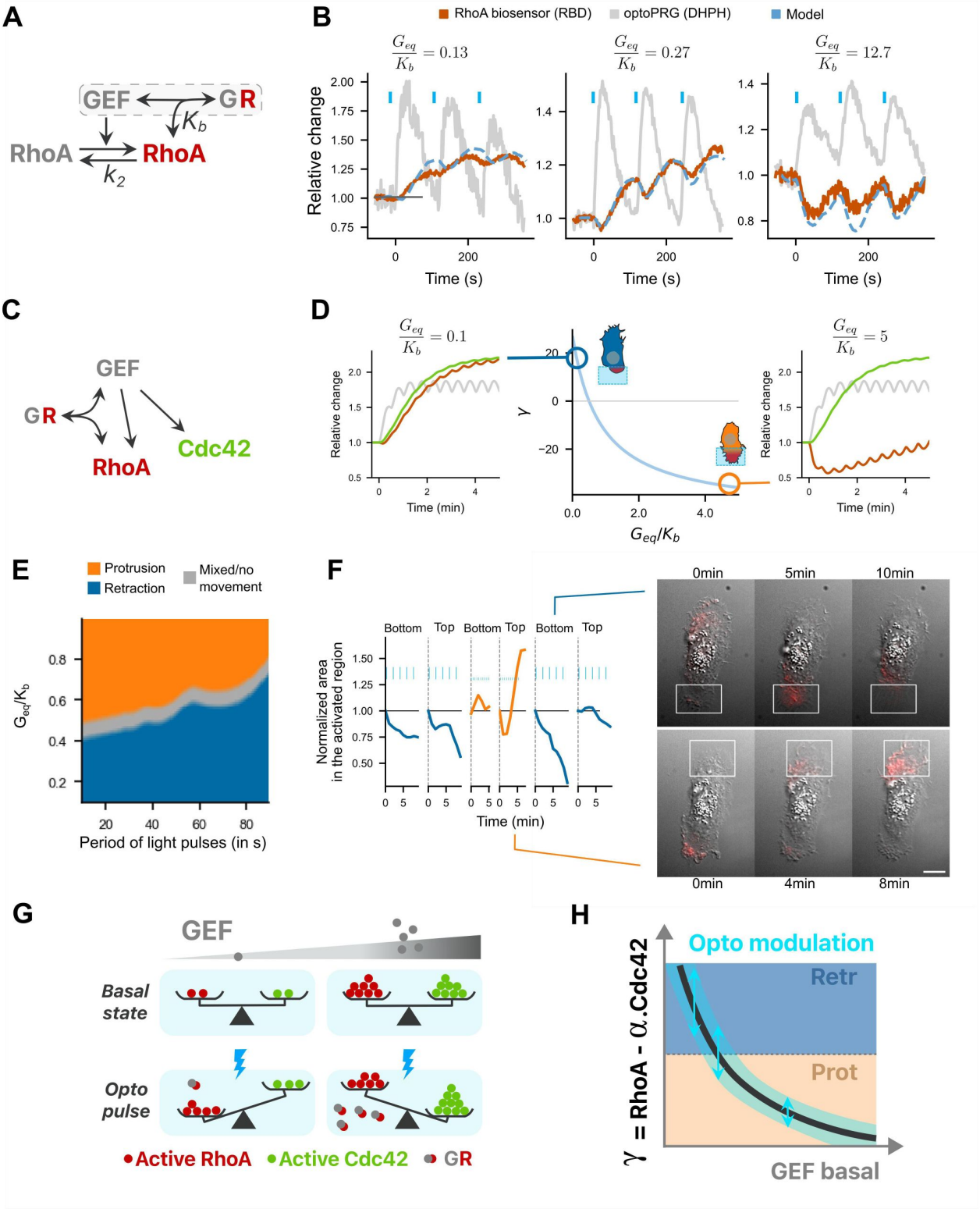
A
GEF
GR
K_b
RhoA
RhoA
k_2
B
RhoA biosensor (RBD)
optoPRG (DHPH)
Model
$\frac{G_{eq}}{K_b} = 0.13$
$\frac{G_{eq}}{K_b} = 0.27$
$\frac{G_{eq}}{K_b} = 12.7$
Relative change
Time (s)
C
GEF
GR
Cdc42
RhoA
D
$\frac{G_{eq}}{K_b} = 0.1$
$\frac{G_{eq}}{K_b} = 5$
Relative change
Time (min)
γ
G_{eq}/K_b
E
Protrusion
Retraction
Mixed/no movement
G_{eq}/K_b
Period of light pulses (in s)
F
Bottom
Top
Normalized area in the activated region
Time (min)
0min
5min
10min
0min
4min
8min
G
GEF
Basal state
Opto pulse
Active RhoA
Active Cdc42
GR
H
Opto modulation
Retr
Prot
γ = RhoA - α.Cdc42
GEF basal

Figure 6

a minimal model recapitulates RhoA activity dynamics and the phenotypic switch.

(**A**) Model for active RhoA dynamics. Interactions are represented with arrows, with the two main parameters of the model. (**B**) The three different RhoA dynamics are well fitted with one single free parameter, G_{eq}/K_b. Dotted blue line: fitted curve, with gray line $g(t)$ taken as input (optoPRG recruitment). Red line: RBD biosensor. (**C**) Complete model, adding Cdc42 to (A): the GEF PRG can activate both RhoA and Cdc42, but can also inhibit RhoA by directly binding to it. (**D**) Center, evolution of γ describing the phenotype (positive for retraction and negative for protrusion) against the free parameter G_{eq}/K_b. Two representative dynamics are shown on the right and on the left for the same input $g(t)$, for a low and high G_{eq}/K_b. In grey, optoPRG recruitment to the membrane, in green, Cdc42 activity, in red, RhoA activity. (**E**) Map of the phenotype as function of the free parameter G_{eq}/K_b and of the duration time between two pulses. (**F**) One example of two phenotypes controlled in the same cell. On the left, first ten minutes of the cell area in the illuminated region for different frequencies and intensities of activation (low frequency high power every 30s, high frequency low power every 15s). On the right, two representative timelapse of retraction (top) and protrusion (bottom), activation is shown with the white rectangle. Scale bar: 10µm. (**G**,**H**) Graphical conclusion on the model. (H) Balance between RhoA and Cdc42 activity is represented in function of GEF basal concentration (grey gradient), both at the basal state (top) and after optogenetic activation (bottom, with blue lightning). At low concentrations RhoA takes over. At high concentration, optoPRG binds to active RhoA and inhibits it (complex *GR*), which enables Cdc42 to take over. (I) Curve showing the difference between RhoA and Cdc42 activity as a function of the basal intensity of the GEF. Phenotypes are marked with the colors (blue, retraction and orange, protrusion). Optogenetic modulation happens on vertical line, with the blue range, which limits the possibility of switching from one phenotype to the other.

This equation, which predicts the temporal evolution of active and free RhoA, r, for any given time dependent GEF curve, g, can be solved numerically and depends on only two variables, k_2 and G_{eq}/K_b. The first variable k_2 can be independently estimated from optogenetic experiments with low amounts of optoPRG, for which the formation of the complex is negligible. By first estimating the kinetics of the RBD biosensor that binds RhoA-GTP (k_{off} = 0.08 ± 0.4 s^{-1}), we found that k_2 = 0.014 ± 0.003 s^{-1} (Supp Note). We are left with only one free parameter, G_{eq}/K_b, which characterizes the basal level of expression of the optoPRG with respect to the typical concentration at which the complex *GR* forms. This parameter changes from cell to cell, depending on the transfection efficiency. Remarkably, we could reproduce the whole family of RhoA dynamics shown in **Figure 4A** adjusting this single parameter (**Figure 6B**), even if not all experimentally observed curves (Supp Figure 4A), probably because our model lacks an auto-amplification process. Despite its limitation and the fact that we assumed identical cell composition (no change of gene expression apart from PRG basal levels), we can consider the model describing RhoA response to optoPRG recruitment as a good representation of biochemical reactions happening in the cell at both low and high concentrations of optoPRG.

To model the phenotype, we next added the activation of Cdc42 by the GEF (**Figure 6C**). To keep our model as simple as possible, we assumed that the deactivation rate of Cdc42 was equal to k_2. We further hypothesized that the binary phenotype observed at the level of membrane dynamics was the outcome of a competition between the retraction protein network triggered by RhoA (involving ROCK, myosin, mDia, and bundled actin) and the protrusion protein network triggered by Cdc42 (involving PAK, Rac, ARP2/3, and branched actin), both of which may involve numerous feedbacks and crosstalks among effectors and regulators on a timescale of few minutes. We modeled this competition by a single number γ, which computes the relative difference between integrated activities of RhoA and Cdc42 during the two first minutes after activation – approximately the time at which the phenotype is experimentally seen. As we have access to relative amounts only, we arbitrarily set the relative contribution of RhoA versus Cdc42 such that when γ is positive the cell retracts, and when negative the cell protrudes. We added a gray zone

around γ =0 (or equivalently when G_{eq}/K_b ~0.5) to take into account the mixed phenotypes. The **Figure 6D** shows the dependence of γ as a function of G_{eq}/K_b. The curve is monotically decreasing: at low G_{eq}/K_bRhoA and Cdc42 dynamics are almost identical but since the cell retracts we assumed that RhoA dominates Cdc42; at high G_{eq}/K_b RhoA is transiently inhibited by the formation of the complex and Cdc42 can dominate leading to a protrusion (see Supp Note).

Having in hands an effective model of the phenotype, we could then explore all possible temporal patterns of activation that correspond to a family of functions $g(t)$. Given the experimental constraints of our optogenetic tool, we focused on the frequency and duration of the light pulses while taking the observed values for *on* and *off* dynamics of the iLID-SspB recruitment. We first looked at the impact of the duration of the pulse, which influences the fold increase of the function g after one pulse of activation. Experimentally, we could go from a fold increase of 1.1 (to be measurable) up to 3. In our model, no cell was able to switch from retracting to protruding or vice versa by only changing the intensity of the optogenetic pulse (Supp Figure 4B). This can be understood by the linearity of the model in which all terms are scaling proportionally to the intensity of the input. Then, we looked at the influence of the frequency of the light pulses on the phenotype. Interestingly, for intermediate values of G_{eq}/K_b ~0.5 we found that high frequencies lead to protruding phenotypes while low frequencies lead to retracting ones (**Figure 6E**). This results from the difference in reaction dynamics: sequestration of RhoA by the PH happens almost instantaneously, while activation of RhoA comes with a delay. This result suggests that one could switch the phenotype in a single cell by selecting it for an intermediate expression level of the optoPRG. To verify this theoretical prediction, we automatically screened cells that expressed optoPRG at a level corresponding to the transition from one phenotype to the other (14-35 a.u., see **Figure 2A**). While the majority of cells showed mixed phenotypes irrespectively of the activation pattern, in very few cells (3 out of 90) we were able to alternate the phenotype between retraction and protrusion several times at different places of the cell by changing the frequency while keeping the same total integrated intensity (**Figure 6F** and Supp Movie X).

Our model can be summarized by the following picture (**Figure 6G**). At low concentration of the GEF, both RhoA and Cdc42 are activated by optogenetic recruitment of optoPRG, but RhoA takes over. At high GEF concentration, recruitment of optoPRG lead to both activation of Cdc42 and inhibition of already present activated RhoA, which pushes the balance towards Cdc42. In the end (**Figure 6H**), optogenetic modulation of PRG can be seen as moving the balance between RhoA and Cdc42 depending on the basal state. This means that only the cells in good concentration range can use the same protein to control both antagonist responses.

Discussion

Using the DH-PH domain of PRG, we have shown that its local recruitment to the plasma membrane can result in two opposite phenotypes: a protrusion in the activation region when highly expressed, or a retraction in the activation region when expressed at low concentrations. The known ability of the DH-PH domain to activate RhoA was confirmed in the case of retraction phenotypes. However, in protruding phenotypes, it negatively regulated RhoA activity in the first minutes after optogenetic perturbations and simultaneously activated Cdc42. These findings were summarized in a simple model that recapitulated the various experimental results. It predicted that cells with intermediate concentrations of the optogenetic actuator could show both phenotypes depending on the frequency of the light pulses. We verified experimentally that it was the case, confirming that we had captured the main features of the underlying biochemical network.

The ability of PRG to induce the two phenotypes is supported by previously reported direct interactions. First and most obviously, the activation of RhoA by the he DH-PH domain of PRG has been well documented, the structure of the complex is even known [25]. The ability of PRG DH-PH

to greatly enhance RhoA-GDP switch to RhoA-GTP has been studied *in vitro* with purified proteins [26]. This enhancement is assumed to come from the positive feedback loop by which RhoA in its active GTP form recruits the GEF through its interaction with the PH domain [18], leading to more activation of RhoA. However, this feedback loop can turn into a negative one for high level of GEF: the direct interaction between the PH domain and RhoA-GTP prevents RhoA-GTP binding to effectors through a competition for the same binding site. Along this line, it was shown that overexpressing the PH domain alone reduced RhoA activity [18]. Second, the direct interaction of the DH-PH domain of PRG with Cdc42-GDP and its ability to enhance the switch to Cdc42-GTP has been shown in a previous work [22]. Notably, the linker region between the DH and the PH domain is required for effective interaction, as well as $G_{\alpha s}$ activity.

Our observation of the double phenotype appeared to be a relatively general feature since we obtained it in another cell line and with at least one other GEF of RhoA. However, the protruding phenotype happened rarely with the DH-PH domain of GEF-H1, and we could not observe it at all with the DH-PH of LARG, another GEF of RhoA from the Dbl family. Thus, the precise biochemical natures of GEF domains are of importance. The interactions of the PH domain of GEF-H1 and LARG with RhoA-GTP have been described in [27]: GEF-H1 PH domain has almost the same inhibition ability as PRG PH domain, while LARG PH domain is less efficient. Moreover, it seems that LARG DH-PH domain has no effect on Cdc42 [22], while nothing is known for GEF-H1 DH-PH domain. As a consequence, the fact that PRG DH-PH is able to trigger protrusions reproducibly compared to other GEFs could be explained by its ability to efficiently inhibit RhoA-GTP while activating Cdc42 at the same time. These two combined properties would allow the GEF to be expressed at a high basal level required for the protruding phenotype since the inhibition by the PH domain prevents RhoA overactivation and Cdc42 activation prevents cell rounding through its competition with RhoA. This could also explain the increase in cell size for protruding cells. Supporting this hypothesis, we observed that expressing transiently optoGEF-H1 and optoLARG was much harder than for optoPRG, many cells becoming round or dying when positively transfected. This underlines the attention that needs to be paid to the choice of specific GEF domains when using optogenetic tools. Tools using DH-PH domains of PRG have been widely used, both in mammalian cells and in Drosophila (with the orthologous gene RhoGEF2), and have been shown to be toxic in some contexts *in vivo*[28]. Our study confirms the complex behavior of this domain which cannot be reduced to a simple RhoA activator.

Interestingly, PRG is known for its role in cell migration, both at the rear [29] and at the front [24]. Given that FRET measurements that are sensing GEFs activity reports RhoA activity at the protruding front [7] and biosensors of RhoA-GTP reports activity at the retracting back [21], our results might solve this paradox: PRG would activate Cdc42 at the front meanwhile activating RhoA at the back. PRG is also known for being prometastatic and is overexpressed in different cancers favoring migration and epithelial to mesenchymal transition [30–32]. In these pathological cases, PRG was studied as a promoter of RhoA activity. However, our results point clearly towards a possible switch in PRG role when overexpressed, acting more on Cdc42 activity. Such a switch in function could be a mechanism happening for other GEFs or proteins and should be considered when designing therapies.

We demonstrated that changing the dynamics of one single protein is enough to revert its function when being recruited to the membrane. Even if the context was quite specific (cells with a specific concentration), such multiplexing may be happening in vivo, where dynamics and local concentrations can highly vary in the cytoplasm and in different subcellular domains. We were limited here by the dynamic of the optogenetic dimer, but our model suggests that optogenetic tools with a shorter lifetime than iLID/SSPB (~20s) would ease the phenotypic switch in the same cell. Similarly, kinetics of endogenous interactions might be tuned on fast timescales by natural molecular circuitries, allowing cells to multiplex signals by this mean. The fact that a protein can have different functions based on its dynamics is not new (Purvis et al. Cell 2013). However, examples that demonstrate a causal relationship between activation of a protein and opposite

cellular responses exist mostly at the transcriptional level, on the timescale of hours [33]. To our knowledge, there are only two examples, both involving optogenetics, of such a dual response on shorter time scales and for protein-protein interactions. In the first example, it was shown that two different acto-adhesive structures could form in response to either Src recruitment or clustering [34]; the specificity being encoded here by the dynamics of Src nanoclusters at the adhesive sites. In the second example, RhoA activation by uncaging of a GEF of RhoA triggered focal adhesion growth via Src activation only at submaximal levels, revealing a selection of cellular response by signal amplitude [19].

Altogether, we have revealed and explained a striking example of protein multiplexing, while underscoring the crucial role of protein dynamics for signal transduction. We have also raised open questions about the link between signaling proteins and their functions, particularly in contexts where they are highly overexpressed, as often observed in cancer.

Acknowledgements

The work was done with support from the LabEx Cell(n)Scale (ANR-10-LABX-0038), Labex and Equipex IPGG (ANR-10-NANO0207), Idex Paris Science et Lettres (ANR-10-IDEX-0001-02 PSL), French National Research Infrastructure France-BioImaging (ANR-10-INBS-04), Institut Convergences Q-life (ANR-17-CONV-0005). JDS thanks AMX from Ecole Polytechnique and the ARC foundation.

Declaration of Interests

The authors declare no competing interests.

Material and methods

Cell culture

hTERT RPE1 cells (CRL-4000 strain, ATCC, Manassas, VA) were cultured at 37°C with 5% CO2 in Dulbecco's modified Eagle's/F-12 medium supplemented with 10% fetal bovine serum, GlutaMAX (2 mM) and penicillin (100 U/mL)-streptomycin (0.1 mg/mL). Cells were passaged twice a week in a ratio of 1/10 by washing them with PBS (1X) solution and dissociating using TrypLE Express (Thermo Fisher Scientific, Waltham, MA) reagent for 3 to 5 minutes.

Plasmids

dTomato-2xrGBD (Plasmid #129625) (RhoA biosensor), pLL7:Venus-iLID-CAAX (#60411), 2XPDZ-mCherry-Larg(DH) (Plasmid #80407) plasmids were bought from Addgene (Watertown, MA).

pLVX: MRLC-iRFP, pLVX: Lifeact-iRFP pLVX: PBD-iRFP (PAK biosensor) plasmids were made by Simon de Beco (Institut Curie, France). pCMV:PRG(DHPH)-RFPt-SspB-P2A-mVenus-iLID-CAAX is a gift from Alessandra Casano (EMBL). pLL7:PRG(DHPH)-iRFP-SspB-P2A-mVenus-iLID-CAAX was subcloned by Maud Bongaerts (Institut Curie, France) from PRG(DHPH)-CRY2-mCherry and pLL7:VenusiLID-CAAX. pCMV:PRG(PH)-iRFP-SspB-P2A-mVenus-iLID-CAAX was subcloned by Benoit Boulevard (Institut Curie, France) from pCMV:PRG(DHPH)-RFPt-SspB-P2A-mVenusiLID-CAAX. pCMV:PRG(PH)-RFPt-SspB-P2A-mVenus-iLID-CAAX was designed in the lab and synthesized by

Twist Bioscience (Twist Bioscience, San Francisco). Rac1 and Cdc42 biosensors, delCMV-mCherry-3xp67Phox and delCMV-mCherry-WaspGBD respectively, described in [Nanda et al., 2023], were gifts from Leif Dehmelt (Dortmund and Max Planck Institute of Molecular Physiology).

Transfection

Transfections were performed using jetPRIME®versatile DNA/siRNA transfection reagent according to the manufacturer's protocol. Different ratio of plasmid DNA were used depending on the constructs, and a ratio of 2:1 of transfection reagent and DNA. Experiments were performed at least 30 hours after DNA transfection, and 48 hours after siRNA transfection.

Drug assay

For IPA-3 (p21-Activated Kinas Inhibitor III, CAS 42521-82-4, Calbiochem), between 20 to 30 cells were first selected and optogenetically activated for 30 minutes. 30 minutes after the end of the first activation, the medium was replaced by the drug diluted in complete DMEM/F-12 medium at specified concentrations, and optogenetic activation was done again five minutes after medium replacement.

Imaging

Imaging was performed at 37 °C in 5% CO2. Two different microscopes have been used: an IX83 and an IX71 (Olympus, Melville, NY) both with inverted fluorescence and Differential Interference Contrast (DIC) and controlled with MetaMorph software (Molecular Devices, Eugene, OR). Both microscopes were equipped with a 60x objective (NA=1.45), motorized stage and filter wheel with SmartShutter Lambda 10-3 control system (Sutter Instrument Company, Novato, CA), a stage-top incubation chamber with temperature and CO2 control (Pecon, Meyer Instruments, Houston, TX), a laser control system with azimuthal TIRF configuration (iLas2, Roper Scientific,Tucson, AZ). The IX71 was equipped with an ORCA-Flash5.0 V3 Digital CMOS camera (Hamamatsu Photonics K.K., Japan), a z-axis guiding piezo motor (PI, Karlsruhe, Germany) a CRISP autofocus system (ASI, Eugene, OR), and a DMD pattern projection device (DLP Light Crafter, Texas instruments, Dalas, TX), illuminated with a SPECTRA Light Engine (Lumencor, Beaverton, OR) at 440±10 nm. The IX83 has a built-in z-piezo and autofocus, and was equipped with a Evolve EMCCD camera (Photometrics, Tucson, AZ) and a FRAP configuration (iLas2, Roper Scientific, Tucson, AZ).

Local optogenetic illumination

Local illumination was performed thanks to a DMD placed on the optical path. DMD used in the experiments was a DLP4500 with a LC4500 controller from Keynote Photonics (Keynotes Photonics, Allen, TX). The chip has a dimension of 1140 x 912 micromirrors (6161.4µm x 9855µm), able to generate 8-bit grayscale patterns. We generated custom illumination patterns using the DMD and a blue LED illumination source (SPECTRA Light Engine (Lumencor, Beaverton, OR).

Cell finder

To find transfected cells on coverslips with a wide range of fluorescence intensities, working with single cells, we developed a small Python software (Python Software Foundation. Python Language Reference, version 3.9.5.), which we named **Cell finder**, that greatly facilitates the search for transfected cells. This software, available on Github *https://github.com/jdeseze/cellfinder*, scans the entire available area, finds any fluorescent object larger than a predefined size (with a threshold to define what is fluorescent), and produces the resulting list of locations in customized format for the Metamorph imaging software (the version on Github has an option to be used with Micromanager). If the number of cells found is too important, a Python-based GUI interface is used to select only the desired positions based on the image acquired during the search trajectory. It allows seeding cells at low density to scatter them, and still have dozens of transfected cells within one 25mm-coverslip for the experiments.

Image analysis

All image analyses have been done with homemade script, using Python (Python Software Foundation. Python Language Reference, version 3.9.5.) through the napari interface [Chiu and Clack, 2022]. All movies are created with Fiji, as well as picture montages. The kymographs have been done thanks to the *Reslice* function in Fiji, with different linewidths depending on the with of the cell. Quantification have been done thanks to custom plugins for napari imaging software [Chiu and Clack, 2022] developed in the lab and available on github (*https://github.com/jdeseze/napari-intensitymeasurements*). Segmentation used optical flow Farneback algorithm in a similar way than in [Robitaille et al., 2022] for membrane displacement measurement, or classical thresholding of fluorescent channel for intensity measurements.

Data processing

Surface displacement : Surface displacement is the area of the intersection between the activated area and cell segmentation. *Normalization* : Biosensors intensities are calculated the following way. First, background is subtracted. Second, mean intensity in the intersection between activated area and cell segmentation is calculated. Third, this intensity is divided by the mean intensity in the non-activated part of the cell. Fourth the intensity is normalized by the intensity before the optogenetic activation. *Dotplots of intensities* : the normalized curved at the specific timepoints specified in each figures are plotted as swarmplots, with the means. *Images and movies* : for DIC images, raw image is divided by the gaussian-filtered image with a large diameter, from 30 to 50 pixels, to correct for uneven illumination. *Sankey diagrams* : sankey diagrams were done by modifying a python library called pySankey (*https://pypi.org/project/pySankey/*). *Persistence* : persistence was calculated as the ratio between the actual distance from the initial point and the sum of the absolute value of all displacements. *Myosin ratio* : clusters were cut it in half along the x-axis, and the ratio between left (activated) and right (non-activated) part was measured.

Modelling

The modelling was performed with Python software (Python Software Foundation. Python Language Reference, version 3.9.5.). The differential equations were integrated thanks to the *odeint* function from scipy.integrate package, and all the fitted parameters were found by the least squares method, using *fmin_powell* function from scipy.optimize for minimization, which uses Powell minimization's method.

References

1. Ridley A.J., Schwartz M.A., Burridge K., Firtel R.A., Ginsberg M.H., Borisy G., Parsons J.T., Horwitz A.R (2003) **Cell Migration: Integrating Signals from Front to Back** *Preprint* https://doi.org/10.1126/science.1092053

2. Jaffe A.B., Hall A (2005) **Rho GTPases: Biochemistry and biology** *Annu Rev Cell Dev Biol* **21**:247–269 https://doi.org/10.1146/ANNUREV.CELLBIO.21.020604.150721

3. Cherfils J., Zeghouf M (2013) **Regulation of small GTPases by GEFs, GAPs, and GDIs** *Physiol Rev* **93**:269–309 https://doi.org/10.1152/PHYSREV.00003.2012/SUPPL_FILE/TABLES1.PDF

4. Hall, a (1998) **Rho GTPases and the actin cytoskeleton** *Science* **279**:509–514

5. Pertz O (2010) **Spatio-temporal Rho GTPase signaling - where are we now?** *J Cell Sci* **123**:1841–1850 https://doi.org/10.1242/jcs.064345

6. Machacek M., Hodgson L., Welch C., Elliott H., Pertz O., Nalbant P., Abell A., Johnson G.L., Hahn K.M., Danuser G (2009) **Coordination of Rho GTPase activities during cell protrusion** *Nature* **461**:99–103 https://doi.org/10.1038/nature08242

7. Pertz O., Hodgson L., Klemke R.L., Hahn K.M (2006) **Spatiotemporal dynamics of RhoA activity in migrating cells** *Nature* **440**:1069–1072 https://doi.org/10.1038/NATURE04665

8. Worthylake R.A., Lemoine S., Watson J.M., Burridge K (2001) **RhoA is required for monocyte tail retraction during transendothelial migration** *J Cell Biol* **154** https://doi.org/10.1083/JCB.200103048

9. de Beco S., Vaidziulyte K., Manzi J., Dalier F., di Federico F., Cornilleau G., Dahan M., Coppey M. (2018) **Optogenetic dissection of Rac1 and Cdc42 gradient shaping** *Nat Commun* **9** https://doi.org/10.1038/s41467-018-07286-8

10. Vaidžiulytė K., Macé A.S., Battistella A., Beng W., Schauer K., Coppey M (2022) **Persistent cell migration emerges from a coupling between protrusion dynamics and polarized trafficking** *Elife* **11** https://doi.org/10.7554/ELIFE.69229

11. Chandrasekar S., Beach J.R., Oakes P.W (2023) **Shining a light on RhoA: Optical control of cell contractility** *Int J Biochem Cell Biol* **161** https://doi.org/10.1016/J.BIOCEL.2023.106442

12. de Seze J., Gatin J., Coppey M. (2023) **RhoA regulation in space and time** *FEBS Lett* **597**:836–849 https://doi.org/10.1002/1873-3468.14578

13. Guntas G., Hallett R.A., Zimmerman S.P., Williams T., Yumerefendi H., Bear J.E., Kuhlman B (2015) **Engineering an improved light-induced dimer (iLID) for controlling the localization and activity of signaling proteins** *Proceedings of the National Academy of Sciences* **112**:112–117 https://doi.org/10.1073/pnas.1417910112

14. Inaba H., Miao Q., Nakata T (2021) **Optogenetic control of small GTPases reveals RhoA mediates intracellular calcium signaling** *Journal of Biological Chemistry* **296** https://doi.org/10.1016/j.jbc.2021.100290

15. Wagner E., Glotzer M (2016) **Local RhoA activation induces cytokinetic furrows independent of spindle position and cell cycle stage** *J Cell Biol* **213**:641–649 https://doi.org/10.1083/JCB.201603025

16. Kamps D. *et al.* (2020) **Optogenetic Tuning Reveals Rho Amplification-Dependent Dynamics of a Cell Contraction Signal Network** *Cell Rep* **33** https://doi.org/10.1016/J.CELREP.2020.108467

17. Valon L., Marín-Llauradó A., Wyatt T., Charras G., Trepat X (2017) **Optogenetic control of cellular forces and mechanotransduction** *Nat Commun* https://doi.org/10.1038/ncomms14396

18. Chen Z., Medina F., Liu M.Y., Thomas C., Sprang S.R., Sternweis P.C (2010) **Activated RhoA binds to the Pleckstrin Homology (PH) domain of PDZ-RhoGEF, a potential site for autoregulation** *Journal of Biological Chemistry* **285**:21070–21081 https://doi.org/10.1074/JBC.M110.122549/ATTACHMENT/EC2A2BE2-3501-4060-81B7-070F3C1ED161/MMC1.PDF

19. Ju J. *et al.* (2022) **Optical regulation of endogenous RhoA reveals selection of cellular responses by signal amplitude** *Cell Rep* **40** https://doi.org/10.1016/J.CELREP.2022.111080

20. Martin K., Reimann A., Fritz R.D., Ryu H., Jeon N.L., Pertz O (2016) **Spatio-temporal co-ordination of RhoA, Rac1 and Cdc42 activation during prototypical edge protrusion and retraction dynamics** *Scientific Reports* **6**:1–14 https://doi.org/10.1038/srep21901

21. Mahlandt E.K., Arts J.J.G., van der Meer W.J., van der Linden F.H., Tol S., van Buul J.D., Gadella T.W.J., Goedhart J. (2021) **Visualizing endogenous Rho activity with an improved localization-based, genetically encoded biosensor** *J Cell Sci* **134** https://doi.org/10.1242/JCS.258823

22. Castillo-Kauil A., García-Jiménez I., Cervantes-Villagrana R.D., Adame-García S.R., Beltrán-Navarro Y.M., Gutkind J.S., Reyes-Cruz G., Vázquez-Prado J (2020) **Gαsdirectly drives PDZ-RhoGEF signaling to Cdc42** *Journal of Biological Chemistry* **295**:16920–16928 https://doi.org/10.1074/JBC.AC120.015204/ATTACHMENT/F8658DD4-1367-4B5B-920F-899371685E0C/MMC2.PDF

23. Mahlandt E.K., Palacios Martínez S., Arts J.J., Tol S., van Buul J.D., Goedhart J. (2023) **Opto-RhoGEFs, an optimized optogenetic toolbox to reversibly control Rho GTPase activity on a global to subcellular scale, enabling precise control over vascular endothelial barrier strength** *Elife* **12** https://doi.org/10.7554/ELIFE.84364

24. Nanda S., Calderon A., Duong T.-T., Koch J., Sachan A., Xin X., Solouk D., Wu Y.-W., Nalbant P., Dehmelt L (2023) **Crosstalk between Rac and Rho GTPase activity mediated by Arhgef11 and Arhgef12 coordinates cell protrusion-retraction cycles** *bioRxiv* https://doi.org/10.1101/2023.02.20.529203

25. Derewenda U., Oleksy A., Stevenson A.S., Korczynska J., Dauter Z., Somlyo A.P., Otlewski J., Somlyo A. V., Derewenda Z.S (2004) **The Crystal Structure of RhoA in Complex with the DH/PH Fragment of PDZRhoGEF, an Activator of the Ca2+ Sensitization Pathway in Smooth Muscle** *Structure* **12**:1955–1965 https://doi.org/10.1016/J.STR.2004.09.003

26. Gasmi-Seabrook G.M.C., Marshall C.B., Cheung M., Kim B., Wang F., Jang Y.J., Mak T.W., Stambolic V., Ikura M (2010) **Real-time NMR Study of Guanine Nucleotide Exchange and Activation of RhoA by PDZ-RhoGEF** *Journal of Biological Chemistry* **285**:5137–5145 https://doi.org/10.1074/JBC.M109.064691

27. Medina F., Carter A.M., Dada O., Gutowski S., Hadas J., Chen Z., Sternweis P.C (2013) **Activated RhoA Is a Positive Feedback Regulator of the Lbc Family of Rho Guanine Nucleotide Exchange Factor Proteins *** *Journal of Biological Chemistry* **288**:11325–11333 https://doi.org/10.1074/JBC.M113.450056

28. Rich A., Fehon R.G., Glotzer M (2020) **Rho1 activation recapitulates early gastrulation events in the ventral, but not dorsal, epithelium of drosophila embryos** *Elife* **9**:1–22 https://doi.org/10.7554/ELIFE.56893

29. Iwanicki M.P., Vomastek T., Tilghman R.W., Martin K.H., Banerjee J., Wedegaertner P.B., Parsons J.T (2008) **FAK, PDZ-RhoGEF and ROCKII cooperate to regulate adhesion movement and trailing-edge retraction in fibroblasts** *J Cell Sci* **121**:895–905 https://doi.org/10.1242/JCS.020941

30. Struckhoff A.P., Rana M.K., Kher S.S., Burow M.E., Hagan J.L., Del Valle L., Worthylake R.A (2013) **PDZ-RhoGEF is essential for CXCR4-driven breast tumor cell motility through spatial regulation of RhoA** *J Cell Sci* **126**:4514–4526 https://doi.org/10.1242/JCS.132381

31. Du J., Zhu Z., Xu L., Chen X., Li X., Lan T., Li W., Yuan K., Zeng Y (2020) **ARHGEF11 promotes proliferation and epithelial-mesenchymal transition of hepatocellular carcinoma through activation of β-catenin pathway** *Aging* **12**:20235–20250 https://doi.org/10.18632/AGING.103772

32. Ding Z., Dhruv H., Kwiatkowska-Piwowarczyk A., Ruggieri R., Kloss J., Symons M., Pirrotte P., Eschbacher J.M., Tran N.L., Loftus J.C (2018) **PDZ-RhoGEF Is a Signaling Effector for TROY-Induced Glioblastoma Cell Invasion and Survival** *Neoplasia* **20** https://doi.org/10.1016/J.NEO.2018.08.008

33. Toettcher J.E., Weiner O.D., Lim W.A (2013) **Using optogenetics to interrogate the dynamic control of signal transmission by the Ras/Erk module** *Cell* **155**:1422–1434 https://doi.org/10.1016/j.cell.2013.11.004

34. Kerjouan A. *et al.* (2021) **Control of SRC molecular dynamics encodes distinct cytoskeletal responses by specifying signaling pathway usage** *J Cell Sci* **134** https://doi.org/10.1242/JCS.254599

Author information

Jean De Seze
Laboratoire Physico Chimie Curie, Institut Curie, PSL Research University, Sorbonne Université, CNRS UMR168, Paris, France
ORCID iD: 0000-0002-6183-4303

Maud Bongaerts
Laboratoire Physico Chimie Curie, Institut Curie, PSL Research University, Sorbonne Université, CNRS UMR168, Paris, France

Benoit Boulevard
Laboratoire Physico Chimie Curie, Institut Curie, PSL Research University, Sorbonne Université, CNRS UMR168, Paris, France

Mathieu Coppey
Laboratoire Physico Chimie Curie, Institut Curie, PSL Research University, Sorbonne Université, CNRS UMR168, Paris, France
ORCID iD: 0000-0001-8924-3233

For correspondence: mathieu.coppey@curie.fr

Editors

Reviewing Editor
Alphee Michelot
Mechanobiology Institute, Singapore, Singapore

Senior Editor
David Ron
University of Cambridge, Cambridge, United Kingdom

Reviewer #1 (Public review):

De Seze et al. investigated the role of guanine exchange factors (GEFs) in controlling cell protrusion and retraction. In order to causally link protein activities to the switch between the opposing cell phenotypes, they employed optogenetic versions of GEFs which can be recruited to the plasma membrane upon light exposure and activate their downstream effectors. Particularly the RhoGEF PRG could elicit both protruding and retracting phenotypes. Interestingly, the phenotype depended on the basal expression level of the optoPRG. By assessing the activity of RhoA and Cdc42, the downstream effectors of PRG, the mechanism of this switch was elucidated: at low PRG levels, RhoA is predominantly activated and leads to cell retraction, whereas at high PRG levels, both RhoA and Cdc42 are activated but PRG also sequesters the active RhoA, therefore Cdc42 dominates and triggers cell protrusion. Finally, they create a minimal model that captures the key dynamics of this protein interaction network and the switch in cell behavior.

The conclusions of this study are strongly supported by data, harnessing the power of modelling and optogenetic activation. The minimal model captures well the dynamics of RhoA and Cdc42 activation and predicts that by changing the frequency of optogenetic activation one can switch between protruding and retracting behaviour in the same cell of intermediate optoPRG level. The authors are indeed able to demonstrate this experimentally albeit with a very low number of cells. A major caveat of this study is that global changes due to PRG overexpression cannot be ruled out. Also, a quantification of absolute protein concentration, which is notoriously difficult, would be useful to put the level of overexpression here in perspective with endogenous levels. Furthermore, it remains unclear whether in cases of protein overexpression in vivo such as cancer, PRG or other GEFs can activate alternative migratory behaviours.

Previous work has implicated RhoA in both protrusion and retraction depending on the context. The mechanism uncovered here provides a convincing explanation for this conundrum. In addition to PRG, optogenetic versions of two other GEFs, LARG and GEF-H1, were used which produced either only one phenotype or less response than optoPRG, underscoring the functional diversity of RhoGEFs. The authors chose transient transfection to achieve a large range of concentration levels and, to find transfected cells at low cell density, developed a small software solution (Cell finder), which could be of interest for other researchers.

https://doi.org/10.7554/eLife.93180.2.sa2

Reviewer #2 (Public review):

Summary:

This manuscript builds from the interesting observation that local recruitment of the DHPH domain of the RhoGEF PRG can induce local retraction, protrusion, or neither. The authors convincingly show that these differential responses are tied to the level of expression of the PRG transgene. This response depends on the Rho-binding activity of the recruited PH domain and is associated with and requires (co?)-activation of Cdc42. This begs the question of why this switch in response occurs. The use a computational model to predict that the timing of protein recruitment can dictate the output of the response in cells expressing intermediate levels and found that, "While the majority of cells showed mixed phenotypes irrespectively of the activation pattern, in few cells (3 out of 90) we were able to alternate the phenotype between retraction and protrusion several times at different places of the cell by changing the frequency while keeping the same total integrated intensity (Figure 6F and Supp Movie)."

Comments on the revised manuscript:

The authors have addressed the previous points and they have convincingly demonstrated that an optogenetically recruited PRG-GEF acts, as expected, as a GEF for RhoA. However, if this fragment is strongly over-expressed, it activates Cdc42, instead of RhoA. This appears to be due to sequestration of active RhoA by the overexpressed PRG-GEF.

https://doi.org/10.7554/eLife.93180.2.sa1

Author response:

The following is the authors' response to the original reviews.

> ***Public Review:***
>
> ***Reviewer #2 (Public Review):***

Regarding reviewer #2 public review, we update here our answers to this public review with new analysis and modification done in the manuscript.

> *This manuscript is missing a direct phenotypic comparison of control cells to complement that of cells expressing RhoGEF2-DHPH at "low levels" (the cells that would respond to optogenetic stimulation by retracting); and cells expressing RhoGEF2-DHPH at "high levels" (the cells that would respond to optogenetic stimulation by protruding). In other words, the authors should examine cell area, the distribution of actin and myosin, etc in all three groups of cells (akin to the time zero data from figures 3 and 5, with a negative control). For example, does the basal expression meaningfully affect the PRG low-expressing cells before activation e.g. ectopic stress fibers? This need not be an optogenetic experiment, the authors could express RhoGEF2DHPH without SspB (as in Fig 4G).*

Updated answer: We thank reviewer #2 for this suggestion. PRG-DHPH overexpression is known to affect the phenotype of the cell as shown in Valon et al., 2017. In our experiments, we could not identify any evidence of a particular phenotype before optogenetic activation apart from the area and spontaneous membrane speed that were already reported in our manuscript (Fig 2E and SuppFig 2). Regarding the distribution of actin and myosin, we did not observe an obvious pattern that will be predictive of the protruding/retracting phenotype.

Trying to be more quantitative, we have classified (by eye, without knowing the expression level of PRG nor the future phenotype) the presence of stress fibers, the amount of cortical actin, the strength of focal adhesions, and the circularity of cells. As shown below, when these classes are binned by levels of expression of PRG (two levels below the threshold and two above) there is no clear determinant. Thus, we concluded that the main driver of the phenotype was the PRG basal expression rather than any particularity of the actin cytoskeleton/cell shape.

Author response image 1.

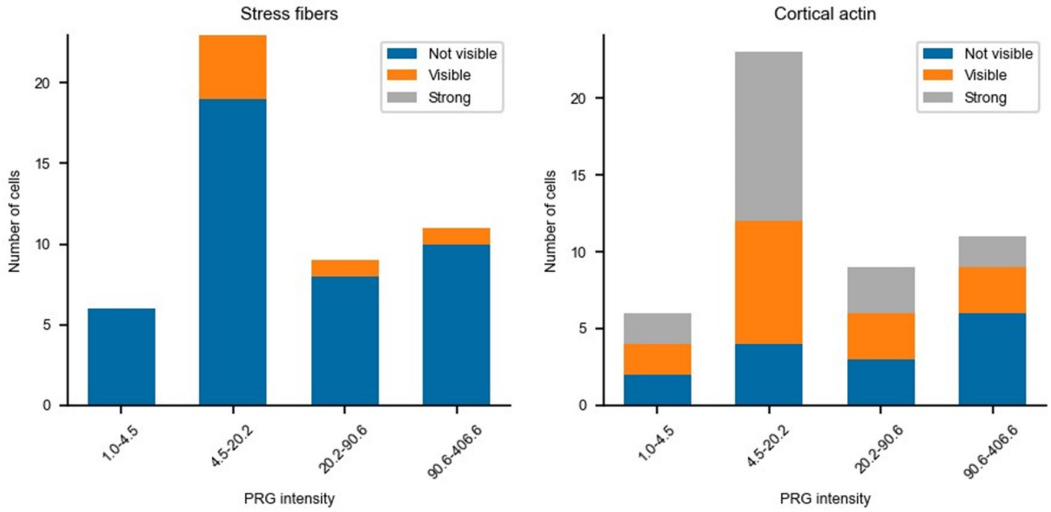

Author response image 2.

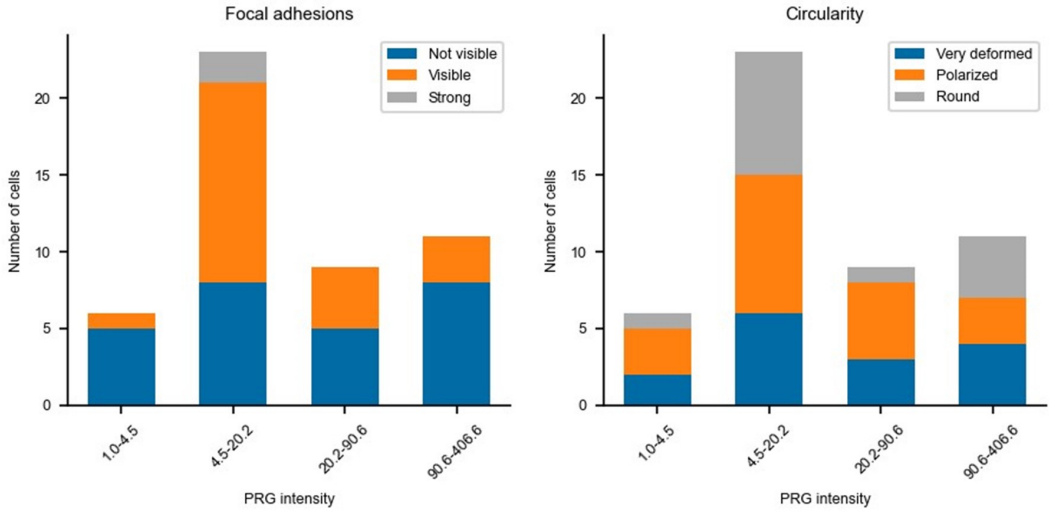

> *Relatedly, the authors seem to assume ("recruitment of the same DH-PH domain of PRG at the membrane, in the same cell line, which means in the same biochemical environment." supplement) that the only difference between the high and low expressors are the level of expression. Given the chronic overexpression and the fact that the capacity for this phenotypic shift is not recruitmentdependent, this is not necessarily a*

> *safe assumption. The expression of this GEF could well induce e.g. gene expression changes.*

Updated answer: We agree with reviewer #2 that there could be changes in gene expression. In the next point of this supplementary note, we had specified it, by saying « that overexpression has an influence on cell state, defined as protein basal activity or concentration before activation. » We are sorry if it was not clear, and we changed this sentence in the revised manuscript (in red in the supp note).

One of the interests of the model is that it does not require any change in absolute concentrations, beside the GEF. The model is thought to be minimal and fits well and explains the data with very few parameters. We do not show that there is no change in concentration, but we show that it is not required to invoke it. We revised a sentence in the new version of the manuscript to include this point.

Additional answer: During the revision process, we have been looking for an experimental demonstration of the independence of the phenotypic switch to any change in global gene expression pattern due to the chronic overexpression of PRG. Our idea was to be in a condition of high PRG overexpression such that cells protrude upon optogenetic activation, and then acutely deplete PRG to see if cells where then retracting. To deplete PRG in a timescale that prevent any change of gene expression, we considered the recently developed CATCHFIRE (PMID: 37640938) chemical dimerizer. We designed an experiment in which the PRG DH-PH domain was expressed in fusion with a FIRE-tag and co-expressing the FIRE-mate fused to TOM20 together with the optoPRG tool. Upon incubation with the MATCH small molecule, we should be able to recruit the overexpressed PRG to the mitochondria within minutes, hereby preventing it to form a complex with active RhoA in the vicinity of the plasma membrane. Unfortunately, despite of numerous trials we never achieved the required conditions: we could not have cells with high enough expression of PRGFIRE-tag (for protrusive response) and low enough expression of optoPRG (for retraction upon PRGFIRE-tag depletion). We still think this would be a nice experiment to perform, but it will require the establishment of a stable cell line with finely tuned expression levels of the CATCHFIRE system that goes beyond the timeline of our present work.

> *Concerning the overall model summarizing the authors' observations, they "hypothesized that the activity of RhoA was in competition with the activity of Cdc42"; "At low concentration of the GEF, both RhoA and Cdc42 are activated by optogenetic recruitment of optoPRG, but RhoA takes over. At high GEF concentration, recruitment of optoPRG lead to both activation of Cdc42 and inhibition of already present activated RhoA, which pushes the balance towards Cdc42."*
>
> *These descriptions are not precise. What is the nature of the competition between RhoA and Cdc42? Is this competition for activation by the GEFs? Is it a competition between the phenotypic output resulting from the effectors of the GEFs? Is it competition from the optogenetic probe and Rho effectors and the Rho biosensors? In all likelihood, all of these effects are involved, but the authors should more precisely explain the underlying nature of this phenotypic switch. Some of these points are clarified in the supplement, but should also be explicit in the main text.*

Updated answer: We consider the competition between RhoA and Cdc42 as a competition between retraction due to the protein network triggered by RhoA (through ROCK-Myosin and mDia-bundled actin) and the protrusion triggered by Cdc42 (through PAK-Rac-ARP2/3-branched Actin). We made this point explicit in the main text.

> ***Recommendations for the authors:***
>
> ***Reviewer #1 (Recommendations For The Authors):***
>
> *Major*
>
> *- why this is only possible for such few cells. Can the authors comment on this in the discussion? Does the model provide any hints?*

As said in our answer to the public comment or reviewer #1, we think that the low number of cells being able to switch can be explained by two different reasons:

(1) First, we were looking for clear inversions of the phenotype, where we could see clear ruffles in the case of the protrusion, and clear retractions in the other case. Thus, we discarded cells that would show in-between phenotypes, because we had no quantitative parameter to compare how protrusive or retractile they were. This reduced the number of switching cells

(2) Second, we had a limitation due to the dynamic of the optogenetic dimer used here. Indeed, the control of the frequency was limited by the dynamic of unbinding of the optogenetic dimer. This dynamic of recruitment (~20s) is comparable to the dynamics of the deactivation of RhoA and Cdc42. Thus, the differences in frequency are smoothed and we could not vary enough the frequency to increase the number of switches. Thanks to the model, we can predict that increasing the unbinding rate of the optogenetic tool (shorter dimer lifetime) should allow us to increase the number of switching cells.

We have added a sentence in the discussion to make this second point explicit.

> *- I would encourage the authors to discuss this molecular signaling switch in the context of general design principles of switches. How generalizable is this network/mechanism? Is it exclusive to activating signaling proteins or would it work with inhibiting mechanisms? Is the competition for the same binding site between activators and effectors a common mechanism in other switches?*

The most common design principle for molecular switches is the bistable switch that relies on a nonlinear activation (for example through cooperativity) with a linear deactivation. Such a design allows the switch between low and high levels. In our case, there is no need for a non-linearity since the core mechanism is a competition for the same binding site on active RhoA of the activator and the effectors. Thus, the design principle would be closer to the notion of a minimal “paradoxical component” (PMID: 23352242) that both activate and limit signal propagation, which in our case can be thought as a self-limiting mechanism to prevent uncontrolled RhoA activation by the positive feedback. Yet, as we show in our work, this core mechanism is not enough for the phenotypic switch to happen since the dual activation of RhoA and Cdc42 is ultimately required for the protrusion phenotype to take over the retracting one. Given the particularity of the switch we observed here, we do not feel comfortable to speculate on any general design principles in the main text, but we thank reviewer #1 for his/her suggestion.

> *- Supplementary figures - there is a discrepancy between the figures called in the text and the supplementary files, which only include SF1-4.*

We apologize for this error and we made the correction.

> *- In the text, the authors use Supp Figure 7 to show that the phenotype could not be switched by varying the fold increase of recruitment through changing the*

> *intensity/duration of the light pulse. Aside from providing the figure, could you give an explanation or speculation of why? Does the model give any prediction as to why this could be difficult to achieve experimentally (is the range of experimentally feasible fold change of 1.1-3 too small? Also, could you clarify why the range is different than the 3 to 10-fold mentioned at the beginning of the results section?*

We thank the reviewer for this question, and this difference between frequency and intensity can be indeed understood in a simple manner through the model.

All the reactions in our model were modeled as linear reactions. Thus, at any timepoint, changing the intensity of the pulse will only change proportionally the amount of the different components (amount of active RhoA, amount of sequestered RhoA, and amount of active Cdc42). This explains why we cannot change the balance between RhoA activity and Cdc42 activity only through the pulse strength. We observed the same experimentally: when we changed the intensity of the pulses, the phenotype would be smaller/stronger, but would never switch, supporting our hypothesis on the linearity of all biochemical reactions.

On the contrary, changing the frequency has an effect, for a simple reason: the dynamics of RhoA and Cdc42 activation are not the same as the dynamics of inhibition of RhoA by the PH domain (see

Figure 4). The inhibition of RhoA by the PH is almost instantaneous while the activation of RhoGTPases has a delay (sets by the deactivation parameter k_2). Intuitively, increasing the frequency will lead to sustained inhibition of RhoA, promoting the protrusion phenotype. Decreasing the frequency – with a stronger pulse to keep the same amount of recruited PRG – restricts this inhibition of RhoA to the first seconds following the activation. The delayed activation of RhoA will then take over.

We added two sentences in the manuscript to explain in greater details the difference between intensity and frequency.

Regarding the difference between the 1.3-3 fold and the 3 to 10 fold, the explanation is the following: the 3 to 10 fold referred to the cumulative amount of proteins being recruited after multiple activations (steady state amount reached after 5 minutes with one activation every 30s); while the 1.3-3 fold is what can be obtained after only one single pulse of activation.

> *- The transient expression achieves a large range of concentration levels which is a strength in this case. To solve the experimental difficulties associated with this, i.e. finding transfected cells at low cell density, the authors developed a software solution (Cell finder). Since this approach will be of interest for a wide range of applications, I think it would deserve a mention in the discussion part.*

We thank the reviewer for his/her interest in this small software solution.

We developed the description of the tool in the Method section. The Cell finder is also available with comments on github (https://github.com/jdeseze/cellfinder) and usable for anyone using Metamorph or Micromanager imaging software.

> *Minor*
>
> *- Can the authors describe what they mean with "cell state"? It is used multiple times in the manuscript and can be interpreted as various things.*

We now explain what we mean by ‘cell state’ in the main text :

“protein basal activities and/or concentrations - which we called the cell state”

> *- “(from 0% to 45%, Figure 2D)", maybe add here: "compare also with Fig. 2A".*

We completed the sentence as suggested, which clarifies the data for the readers.

> *- The sentence "Given that the phenotype switch appeared to be controlled by the amount of overexpressed optoPRG, we hypothesized that the corresponding leakiness of activity could influence the cell state prior to any activation." might be hard to understand for readers unfamiliar with optogenetic systems. I suggest adding a short sentence explaining dark-state activity/leakiness before putting the hypothesis forward.*

We changed this whole beginning of the paragraph to clarify.

> *- Figure 2E and SF2A. I would suggest swapping these two panels as the quantification of the membrane displacement before activation seems more relevant in this context.*

We thank reviewer #1 for this suggestion and we agree with it (we swapped the two panels)

> *- Fig. 2B is missing the white frames in the mixed panels.*

We are sorry for this mistake, we changed it in the new version.

> *- In the text describing the experiment of Fig. 4G, it would again be helpful to define what the authors mean by cell state, or to state the expected outcome for both hypotheses before revealing the result.*

We added precisions above on what we meant by cell state, which is the basal protein activities and/or concentrations prior to optogenetic activation. We added the expectation as follow:

To discriminate between these two hypotheses, we overexpressed the DH-PH domain alone in another fluorescent channel (iRFP) and recruited the mutated PH at the membrane. “If the binding to RhoA-GTP was only required to change the cell state, we would expect the same statistics than in Figure 2D, with a majority of protruding cells due to DH-PH overexpression. On the contrary, we observed a large majority of retracting phenotype even in highly expressing cells (Figure 4G), showing that the PH binding to RhoA-GTP during recruitment is a key component of the protruding phenotype.”

> *- Figure 4H,I: "of cells that overexpress PRG, where we only recruit the PH domain" doesn't match with the figure caption. Are these two constructs in the same cell? If not please clarify the main text.*

We agree that it was not clear. Both constructs are in the same cell, and we changed the figure caption accordingly.

> *- "since RhoA dominates Cdc42" is this concluded from experiments (if yes, please refer to the figure) or is this known from the literature (if yes, please cite).*

The assumption that RhoA dominates Cdc42 comes from the fact that we see retraction at low PRG concentration. We assumed that RhoA is responsible for the retraction phenotype. Our assumption is based on the literature (Burridge 2004 as an example of a review, confirmed by many experiments, such as the direct recruitment of RhoA to the membrane, see Berlew 2021) and is supported by our observations of immediate increase of RhoA activity at low PRG. We modified the text to clarify it is an assumption.

> *- Fig. 6G o left: is not intuitive, why are the number of molecules different to start with?*

The number of molecules is different because they represent the active molecules: increasing the amount of PRG increases the amount of active RhoA and active Cdc42. We updated the figure to clarify this point.

> *o right: the y-axis label says "phenotype", maybe change it to "activity" or add a second y-axis on the right with "phenotype"?*

We updated the figure following reviewer #1 suggestion.

> *- Discussion: "or a retraction in the same region" sounds like in the same cell. Perhaps rephrase to state retraction in a similar region?*

Sorry for the confusion, we change it to be really clear: *"a protrusion in the activation region when highly expressed, or a retraction in the activation region when expressed at low concentrations."*

> *Typos:*
>
> *- "between 3 and 10 fold" without s.*
>
> *- Fig. 1H, y-axis label.*
>
> *- "whose spectrum overlaps" with s.*
>
> *- "it first decays, and then rises" with s.*
>
> *- Fig 4B and Fig 6B. Is the time in sec or min? (Maybe double-check all figures).*
>
> *- "This result suggests that one could switch the phenotype in a single cell by selecting it for an intermediate expression level of the optoPRG.".*
>
> *- "GEF-H1 PH domain has almost the same inhibition ability as PRG PH domain".*

We corrected all these mistakes and thank the reviewer for his careful reading of the manuscript.

> ***Reviewer #2 (Recommendations For The Authors):***
>
> *Likewise, the model assumes that at high PRG GEF expression, the "reaction is happening far from saturation ..." and that "GTPases activated with strong stimuli -giving rise to strong phenotypic changes- lead to only 5% of the proteins in a GTP-state, both for RhoA and Cdc42". Given the high levels of expression (the absolute value of which is not known) this assumption is not necessarily safe to assume. The shift to Cdc42 could indeed result from the quantitative conversion of RhoA into its active state.*

We agree with the reviewer that the hypothesis that RhoA is fully converted into its active state cannot be completely ruled out. However, we think that the two following points can justify our choice.

- First, we see that even in the protruding phenotype, RhoA activity is increasing upon optoPRG recruitment (Figure 3). This means that RhoA is not completely turned into its active GTP-loaded state. The biosensor intensity is rising by a factor 1.5 after 5 minutes (and continue to increase, even if not shown here). For sure, it could be explained by the

relocation of RhoA to the place of activation, but it still shows that cells with high PRG expression are not completely saturated in RhoA-GTP.

- We agree that linearity (no saturation) is still an hypothesis and very difficult to rule out, because it is not only a question of absolute concentrations of GEFs and RhoA, but also a question of their reaction kinetics, which are unknow parameters *in vivo*. Yet, adding a saturation parameter would mean adding 3 unknown parameters (absolute concentrations of RhoA, as well as two reaction constants). The fact that there are not needed to fit the complex curves of RhoA as we do with only one parameter tends to show that the minimal ingredients representing the interaction are captured here.

> *The observed "inhibition of RhoA by the PH domain of the GEF at high concentrations" could result from the ability of the probe to, upon membrane recruitment, bind to active RhoA (via its PH domain) thereby outcompeting the RhoA biosensor (Figure 4A-C). This reaction is explicitly stated in the supplemental materials ("PH domain binding to RhoA-GTP is required for protruding phenotype but not sufficient, and it is acting as an inhibitor of RhoA activity."), but should be more explicit in the main text. Indeed, even when PRG DHPH is expressed at high concentrations, it does activate RhoA upon recruitment (figure 3GH). Not only might overexpression of this active RhoA-binding probe inhibit the cortical recruitment of the RhoA biosensor, but it may also inhibit the ability of active RhoA to activate its downstream effectors, such as ROCK, which could explain the decrease in myosin accumulation (figure 3D-F). It is not clear that there is a way to clearly rule this out, but it may impact the interpretation.*

This hypothesis is actually what we claim in the manuscript. We think that the inhibition of RhoA by the PH domain is explained by its direct binding. We may have missed what Reviewer #2 wanted to say, but we think that we state it explicitly in the main text :

“Knowing that the PH domain of PRG triggers a positive feedback loop thanks to its binding to active RhoA 18, we hypothesized that this binding could sequester active RhoA at high optoPRG levels, thus being responsible for its inhibition.”

And also in the Discussion:

“However, this feedback loop can turn into a negative one for high levels of GEF: the direct interaction between the PH domain and RhoA-GTP prevents RhoA-GTP binding to effectors through a competition for the same binding site.”

We may have not been clear, but we think that this is what is happening: the PH domain prevents the binding to effectors and decreases RhoA activity (as was shown in Chen et al. 2010).

> *The X-axis in Figure 4C time is in seconds not minutes. The Y-axis in Figure 4H is unlabeled.*

We are sorry for the mistake of Figure 4C. We changed the Y-axis in the Figure 4h.

> *Although this publication cites some of the relevant prior literature, it fails to cite some particularly relevant works. For example, the authors state, "The LARG DH domain was already used with the iLid system" and refers to a 2018 paper (ref 19), whereas that domain was first used in 2016 (PMID 27298323). Indeed, the authors used the plasmid from this 2016 paper to build their construct.*

We thank the reviewer for pointing out this error, we have corrected the citation and put the seminal one in the revised version.

> *An analogous situation pertains to previous work that showed that an optogenetic probe containing the DH and PH domains in RhoGEF2 is somewhat toxic in vivo (table 6; PMID 33200987). Furthermore, it has previously been shown that mutation of the equivalent of F1044A and I1046E eliminates this toxicity (table 6; PMID 33200987) in vivo. This is particularly important because the Rho probe expressing RhoGEF2-DHPH is in widespread usage (76 citations in PubMed). The ability of this probe to activate Cdc42 may explain some of the phenotypic differences described resulting from the recruitment of RhoGEF2-DHPH and LARG-DH in a developmental context (PMID 29915285, 33200987).*

We thank reviewer #2 for these comments, and added a small section in the discussion, for optogenetic users:

This underlines the attention that needs to be paid to the choice of specific GEF domains when using optogenetic tools. Tools using DH-PH domains of PRG have been widely used, both in mammalian cells and in Drosophila (with the orthologous gene RhoGEF2), and have been shown to be toxic in some contexts in vivo 28. Our study confirms the complex behavior of this domain which cannot be reduced to a simple RhoA activator.

> *Concerning the experiment shown in 4D, it would be informative to repeat this experiment in which a non-recruitable DH-PH domain of PRG is overexpressed at high levels and the DH domain of LARG is recruited. This would enable the authors to distinguish whether the protrusion response is entirely dependent on the cell state prior to activation or the combination of the cell state prior to activation and the ability of PRG DHPH to also activate Cdc42.*

We thank the reviewer for his suggestion. Yet, we think that we have enough direct evidence that the protruding phenotype is due to both the cell state prior to activation and the ability of PRG DHPH to also activate Cdc42. First, we see a direct increase in Cdc42 activity following optoPRG recruitment (see Figure 6). This increase is sustained in the protruding phenotype and precedes Rac1 and RhoA activity, which shows that it is the first of these three GTPases to be activated. Moreover, we showed that inhibition of PAK by the very specific drug IPA3 is completely abolishing only the protruding phenotype, which shows that PAK, a direct effector of Cdc42 and Rac1, is required for the protruding phenotype to happen. We know also that the cell state prior to activation is defining the phenotype, thanks to the data presented in Figure 2.

We further showed in Figure 1 that LARG DH-PH domain was not able to promote protrusion. The proposed experiment would be interesting to confirm that LARG does not have the ability to activate another GTPase, even in a different cell state with overexpressed PRG. However, we are not sure it would bring any substantial findings to understand the mechanism we describe here, given the facts provided above.

> *Similarly, as PRG activates both Cdc42 and Rho at high levels, it would be important to determine the extent to which the acute Rho activation contributes to the observed phenotype (e.g. with Rho kinase inhibitor).*

We agree with the reviewer that it would be interesting to know whether RhoA activation contributes to the observed phenotype, and we have tried such experiments.

For Rho kinase inhibitor, we tried with Y-27632 and we could never prevent the protruding phenotype to happen. However, we could not completely abolish the retracting phenotype either (even when the effect on the cells was quite strong and visible), which could be due to other effectors compensating for this inhibition. As RhoA has many other effectors, it does not tell us that RhoA is not required for protrusion.

We also tried with C3, which is a direct inhibitor of RhoA. However, it had too much impact on the basal state of the cells, making it impossible to recruit (cells were becoming round and clearly dying. As both the basal state and optogenetic activation require the activation of RhoA, it is hard to conclude out of experiments where no cell is responding.

> *The ability of PRG to activate Cdc42 in vivo is striking given the strong preference for RhoA over Cdc42 in vitro (2400X) (PMID 23255595). Is it possible that at these high expression levels, much of the RhoA in the cell is already activated, so that the sole effect that recruited PRG can induce is activation of Cdc42? This is related to the previous point pertaining to absolute expression levels.*

As discussed before, we think that it is not only a question of absolute expression levels, but also of the affinities between the different partners. But Reviewer #2 is right, there is a competition between the activation of RhoA and Cdc42 by optoPRG, and activation of Cdc42 probably happens at higher concentration because of smaller effective affinity.

Still, we know that activation of the Cdc42 by PRG DH-PH domain is possible *in vivo*, as it was very clearly shown in Castillo-Kauil et al., 2020 (PMID 33023908). They show that this activation requires the linker between DH and PH domain of PRG, as well as Gαs activation, which requires a change in PRG DH-PH conformation. This conformational switch does not happen *in vitro*, which might explain why the affinity against Cdc42 was found to be very low.

> *Minor points*
>
> *In both the abstract and the introduction the authors state, "we show that a single protein can trigger either protrusion or retraction when recruited to the plasma membrane, polarizing the cell in two opposite directions." However, the cells do not polarize in opposite directions, ie the cells that retract do not protrude in the direction opposite the retraction (or at least that is not shown). Rather a single protein can trigger either protrusion or retraction when recruited to the plasma membrane, depending upon expression levels.*

We thank the reviewer for this remark, and we agree that we had not shown any data supporting a change in polarization. We solved this issue, by showing now in Supplementary Figure 1 the change in areas in both the activated and in the not activated region. The data clearly show that when a protrusion is happening, the cell retracts in the non-activated region. On the other hand, when the cell retracts, a protrusion happens in the other part of the cell, while the total area is staying approximately constant.

We added the following sentence to describe our new figure:

Quantification of the changes in membrane area in both the activated and non-activated part of the cell (Supp Figure 1B-C) reveals that the whole cell is moving, polarizing in one direction or the other upon optogenetic activation.

> *While the authors provide extensive quantitative data in this manuscript and quantify the relative differences in expression levels that result in the different phenotypes, it would be helpful to quantify the absolute levels of expression of these GEFs relative to e.g. an endogenously expressed GEF.*

We agree with the reviewer comment, and we also wanted to have an idea of the absolute level of expression of GEFs present in these cells to be able to relate fluorescent intensities with absolute concentrations. We tried different methods, especially with the purified fluorescent protein, but having exact numbers is a hard task.

We ended up quantifying the amount of fluorescent protein within a stable cell line thanks to ELISA and comparing it with the mean fluorescence seen under the microscope.

We estimated that the switch concentration was around 200nM, which is 8 times more than the mean endogenous concentration according to https://opencell.czbiohub.org/, but should be reachable locally in wild type cell, or globally in mutated cancer cells.

> *Given the numerical data (mostly) in hand, it would be interesting to determine whether RhoGEF2 levels, cell area, the pattern of actin assembly, or some other property is most predictive of the response to PRG DHPH recruitment.*
>
> *We think that the manuscript made it clear that the concentration of PRG DHPH is almost 100% predictive of the response to PRG DHPH. We believe that other phenotypes such as the cell area or the pattern of actin assembly would only be consequences of this. Interestingly, as experimentators we were absolutely not able to predict the behavior by only seeing the shape of the cell, event after hundreds of activation experiments, and we tried to find characteristics that would distinguish both populations with the data in our hands and could not find any.*
>
> *There is some room for general improvement/editing of the text.*

We tried our best to improve the text, following reviewers suggestions.

https://doi.org/10.7554/eLife.93180.2.sa0